Interplay between superconductivity and non-Fermi liquid behavior at a quantum-critical point in a metal. V. The γ model and its phase diagram: The case $\gamma = 2$

Yi-Ming Wu,[1] Shang-Shun Zhang,[1] Artem Abanov,[2] and Andrey V. Chubukov[1]
[1]*School of Physics and Astronomy and William I. Fine Theoretical Physics Institute, University of Minnesota, Minneapolis, Minnesota 55455, USA*
[2]*Department of Physics, Texas A&M University, College Station, Texas 77843, USA*

(Received 8 February 2021; revised 20 April 2021; accepted 21 April 2021; published 13 May 2021)

This paper is a continuation and a partial summary of our analysis of the pairing at a quantum-critical point (QCP) in a metal for a set of quantum-critical systems, whose low-energy physics is described by an effective model with dynamical electron-electron interaction $V(\Omega_m) = (\bar{g}/|\Omega_m|)^\gamma$ (the γ model). Examples include pairing at the onset of various spin and charge-density-wave and nematic orders and pairing in SYK-type models. In previous papers, we analyzed the physics for $\gamma < 2$. We have shown that the onset temperature for the pairing T_p is finite, of order $\bar{g}$, yet the gap equation at $T = 0$ has an infinite set of solutions within the same spatial symmetry. As the consequence, the condensation energy E_c has an infinite number of minima. The spectrum of E_c is discrete, but becomes more dense as γ increases. Here we consider the case $\gamma = 2$. The $\gamma = 2$ model attracted special interest in the past as it describes the pairing by an Einstein phonon in the limit when the dressed phonon mass ω_D vanishes. We show that for $\gamma = 2$, the spectrum of E_c becomes continuous. We argue that the associated gapless "longitudinal" fluctuations destroy superconducting phase coherence at a finite T, such that at $0 < T < T_p$, the system displays pseudogap behavior of preformed pairs. We show that for each gap function from the continuum spectrum, there is an infinite array of dynamical vortices in the upper half-plane of frequency. For the electron-phonon case, our results show that $T_p = 0.1827\bar{g}$, obtained in earlier studies, marks the onset of the pseudogap behavior, while the actual superconducting T_c vanishes at $\omega_D \to 0$.

DOI: 10.1103/PhysRevB.103.184508

I. INTRODUCTION

This work presents a continuation and a partial summary of our analysis of the interplay between non-Fermi liquid (NFL) physics and superconductivity for a set of quantum-critical (QC) itinerant systems, whose low-energy dynamics can be described by an effective model of spin-full electrons with dynamical interaction on the Matsubara axis $V(\Omega_m) = (\bar{g}/|\Omega_m|)^\gamma$ (the γ model). Examples include pairing near spin-density-wave, charge-density-wave, and Ising-nematic instabilities in isotropic and anisotropic 3D and 2D systems, pairing of fermions at a half-filled Landau level, pairing of dispersion-less fermions randomly coupled to phonons, and so on. We listed the examples in the first paper in the series, Ref. [1], and discussed earlier works. In that and subsequent papers [1–4], hereafter called papers I–IV, we analyzed the γ model with exponents $0 < \gamma < 2$. We rationalized Eliashberg-type approach, solved generalized Eliashberg equations, and found that the solution with a nonzero pairing gap develops below a finite T_p, which for a generic $\gamma = O(1)$ is of order $\bar{g}$. The corresponding gap function $\Delta(k, \omega_m)$ can be roughly approximated as $\Delta(\omega_m)f(k)$, where a normalized $f(k)$ has a particular spatial symmetry ($d-$ wave, s^{+-}, etc.), and $\Delta(\omega_m)$ is a sign-preserving function of Matsubara frequency, whose amplitude increases with decreasing T. At $T = 0$, $\Delta(0)$ is of order T_p (the ratio $\Delta(0)/T_p$ is a γ-dependent number [5,6]). In this respect, the pairing at a QCP is similar to pairing away from a QCP, when $V(\Omega_m)$ saturates at a finite value at $\Omega_m = 0$. However, on a more careful look, we found qualitative difference between the two cases. Namely, away from a QCP, Eliashberg gap equation at $T = 0$ has at most a finite number of solutions with a given spatial symmetry. At a QCP, it has an infinite number of solutions for $\Delta(\omega)$, i.e., the condensation energy, E_c, has an infinite number of local minima. The solutions $\Delta_n(\omega_m)$, labeled by an integer n, are topologically distinct in the sense that $\Delta_n(\omega_m)$ changes sign n times along the positive Matsubara axis, and each such point is a vortex in the upper half-plane of frequency.

The ultimate goal of our studies of the γ model is to understand how the existence of an infinite set of solutions affects the interplay between pairing [i.e., the appearance of a nonzero $\Delta(\omega)$] and a true superconductivity. In a conventional Eliashberg theory (ET) of SC out of a noncritical Fermi liquid, phase fluctuations are small in the same parameter that allows one to neglect vertex corrections. In this situation, the onset temperature for the pairing, T_p, and the actual superconducting T_c nearly coincide. To address a possible reduction of superconducting T_c by phase fluctuations, one then has to include the effects not incorporated into ET, e.g., a localization of electrons when the interaction exceeds the fermionic bandwidth. We analyze whether the emergence of an infinite number of solutions for the gap at a QCP gives rise to a substantial reduction of T_c/T_p ratio already when the interaction is smaller than the fermionic bandwidth. For

$\gamma < 2$, which we analyzed in papers I–IV, the spectrum of the condensation energies $E_{c,n}$ is discrete, and $E_{c,0}$ is the largest. In this situation, the physics at small T is determined by a single solution $\Delta_0(\omega_m)$, and phase fluctuations are weak. We showed, however, that the set becomes more dense at γ increases: the ratios $(E_{c,n+1} - E_{c,n})/E_{c,n}$ get progressively smaller.

In this paper, we analyze the case $\gamma = 2$. We argue that for this γ, the set of the gap functions and the spectrum of the condensation energies become continuous. Specifically, at $\gamma = 2 - \delta$, and $\delta = 0+$, $\Delta_n(\omega_m)$ with $n < 1/\delta$ become equal to $\Delta_0(\omega_m)$ for all $\omega_m > 0$, and $E_{c,n}$ become equal to $E_{c,0}$, while $\Delta_n(\omega_m)$ and $E_{c,n}$ with infinite $n > 1/\delta$ form a continuous, one-parameter gapless spectra, $\Delta_\xi(\omega_m)$ and $E_{c,\xi}$. Here ξ, is a continuous variable, that runs between zero and infinity and depends on how the double limit $n \to \infty$ and $\delta \to 0$ is taken (we define ξ such that the minimum of $E_{c,\xi}$ is at $\xi = 0$, and $E_{c,\infty} = 0$). We argue that fluctuation corrections to superconducting order parameter from $E_{c,\xi}$ destroy long-range superconducting order at any finite T. We emphasize that this holds for itinerant fermions, in the limit when the interaction is smaller than the bandwidth, and the ET is rigorously justified.

We present a corroborative evidence that the $\gamma = 2$ model is critical. It comes from the analysis of the gap equation on the real frequency axis and in the upper half-plane of frequency, $z = \omega' + i\omega''$, $\omega'' > 0$. The gap function $\Delta(z)$ generally cannot be obtained from $\Delta(\omega_m)$ by just replacing $i\omega_m$ by z as such gap function is not guaranteed to be analytic. To obtain an analytic function, one has to perform a more sophisticated analysis [7–10]. As a consequence, $\Delta(\omega)$ on the real axis can be quite different from $\Delta(\omega_m)$. For the γ model, some difference is expected on general grounds, particularly for $\gamma > 1$, because while the interaction $V(\Omega_m)$ on the Matsubara axis is positive (attractive) for all γ, the one on the real axis is complex, $V(\Omega) = e^{i\pi\gamma/2\,\mathrm{sgn}\Omega}/|\Omega|^\gamma$, and its real part $V'(\Omega) = (\bar{g}/|\Omega|)^\gamma \cos\pi\gamma/2$ becomes repulsive for $\gamma > 1$.

In paper IV, we compared the forms of $\Delta_n(\omega_m)$ and $\Delta_n(\omega)$ for $1 < \gamma < 2$. We found that at small ω, $\omega_m < \bar{g}$ and at large $\omega, \omega_m > \bar{g}(|\ln(2-\gamma)|/(2-\gamma))^{1/2}$, the two gap functions transfer into each other under a rotation $i\omega_m \to \omega$. However, at intermediate $\bar{g} < \omega, \omega_m < (|\ln(2-\gamma)|/(2-\gamma))^{1/2}$, $\Delta_n(\omega_m) = a_n/|\omega_m|^\gamma$ is a sign-preserving function of frequency, while $\Delta_n(\omega) = |\Delta_n(\omega)|e^{i\eta_n(\omega)}$ oscillates, and its phase $\eta_n(\omega)$ winds up by $2\pi k_\gamma$, where k_γ is an integer, which depends on γ, but not on n. We extended the analysis to complex z in the upper frequency half-plane and showed that there exists an array of k dynamical vortices, centered at some complex z_i.

Here we show that for $\gamma = 2$, the gap functions on the real axis form a continuous set, each $\Delta_\xi(\omega)$ oscillates up to an infinite frequency, and its phase winds up by an infinite number of 2π. Accordingly, the number of vortices at z_i becomes infinite, and the array of z_i extends up to an infinite frequency, where, we argue, each $\Delta_\xi(\omega)$ develops an essential singularity. We show that for each gap function from the set, the density of states (DoS) $N_\xi(\omega + i0)$ has an infinite number of maxima and minima, and does not recover the normal state form up to $\omega = \infty$. For the solution with $\xi = 0$, which was studied before [7–9,11,12], $N(\omega + i0)$ reduces to a set of δ functions at some ω_i.

We combine the results for $\gamma = 2$ and earlier results for $\gamma < 2$ (papers I–IV) and present the phase diagram of the γ model for $\gamma \leqslant 2$, Fig. 16. For all γ, the ground state is a superconductor with a finite superfluid stiffness ρ_s, and the onset temperature for the pairing, T_p, is finite. However, superconducting T_c decreases with γ and vanishes for $\gamma = 2$. In between T_p and T_c, the system displays a pseudogap (preformed pairs) behavior. One feature of this phase is "gap filling" behavior, as T increases towards T_p. In the next paper we consider the case $\gamma > 2$. We show that the behavior at a finite T remains largely the same as for $\gamma = 2$, however new physics emerges at $T = 0$ and gives rise to a reduction and eventual vanishing of ρ_s even in the ground state.

The model with the pairing interaction $V(\Omega_m) = (\bar{g}/|\Omega_m|)^2$ attracted a substantial attention on its own as it describes the pairing, mediated by an Einstein boson, in the limit where the effective (dressed) Debye frequency ω_D vanishes.[1] Electron-phonon model at $\omega_D \to 0$ has been studied before by a large number of authors [7–9,13–16]. We use the results of these studies, particularly the works by Karakozov, Maksimov, and Mikhailovsky [7], Marsiglio and Carbotte [8], and Combescot [9] as the input for some of our calculations. This limit is often termed strong coupling as the dimensionless coupling constant $\lambda = (\bar{g}/\omega_D)^2$ diverges at $\omega_D \to 0$. However, the interaction $\bar{g}$ is still assumed to be smaller than the Fermi energy E_F. Indeed, ET includes contributions to all orders in λ within the ladder approximation, but neglects vertex corrections to ladder series. The latter hold in powers of Migdal-Eliashberg parameter $\lambda_E = \bar{g}^2 N_0/\omega_D = \lambda(N_0\omega_D)$, where $N_0 \sim 1/E_F$ in the DoS per unit volume. For small enough $\bar{g}/E_F$, λ_E remains small even when λ is large. From this perspective, the strong coupling limit of the ET is the double limit in which ω_D and $\bar{g}/E_F$ tend to zero simultaneously, such that λ_E remains small. In physical terms, the smallness of $\lambda_E \ll \lambda$ comes about because in a process that gives rise to a vertex correction, fermions are forced to vibrate at a phonon frequency, far away from their own resonance, while in the processes, which form series in λ, fermions are vibrating near their resonance frequencies. The smallness of λ_E also allows one to neglect the renormalization of the bosonic propagator by fermions, both in the normal and in the superconducting state.

Previous studies have found that a nonzero gap function emerges at $T_p \approx 0.25\omega_D e^{-1/\lambda}$ at weak coupling (Refs. [17–23]) and at $T_p = 0.1827\bar{g}$ at strong coupling [8,9,14,24].[2] To understand the interplay between the onset of pairing and T_c, one has to also compute superfluid stiffness, ρ_s. At weak coupling, $\rho_s \sim E_F \gg T_p$ [25–30]. In this situation, T_c and T_p almost coincide. At strong coupling, the situation is more complex. At $T = 0$, the $\rho_s \sim T_p/\lambda_E$ (see below). Within the validity of ET, this stiffness exceeds T_p. If we were to neglect the continuum

[1]The model also describes strong coupling limit of the interaction between dispersion-less fermions and phonons (SYK-Yukawa model), Refs. [10–12,24].

[2]This formula was originally obtained semi-analytically by Allen and Dynes [14]. They expressed it as $T_p \sim \omega_D\sqrt{\lambda}$ to emphasize that at strong coupling T_p becomes larger than ω_D. Given that $\lambda = (\bar{g}/\omega_D)^2$, their formula reduces to $T_p \sim \bar{g}$.

spectrum of the condensation energy, we would obtain that T_p and T_c again also coincide, as thermal corrections to SC order parameter are of order T/ρ_s and hence remain small for all $T < T_p$. Including the additional corrections from the continuum of $E_{c,\xi}$, we find that thermal corrections actually hold in powers of $T/(\omega_D\lambda_E)$ and become of order one at $T \sim \omega_D\lambda_E$, which we identify with the actual T_c. At small $\omega_D/\bar{g}$, this T_c is much smaller than T_p, even if we set $\lambda_E = O(1)$. In between $T = T_p$ and T_c, the system displays a preformed pairs behavior. When ω_D increases and becomes of order $\bar{g}$, the pseudogap region shrinks and the system gradually recovers BCS-like behavior (Fig. 15).

The structure of the paper is the following. In Sec. II, we present the Eliashberg gap equations that we use in this paper. In Sec. III, we discuss the solution of the gap equation along the Matsubara axis at $T = 0$ and $\gamma \to 2$. We first obtain, in Secs. III A and III B, the exact solution of the linearized gap equation, $\Delta_\infty(\omega_m)$, which changes sign an infinite number of times between $\omega_m = 0$ and $\omega_m \sim \bar{g}$, and sign-preserving solution $\Delta_0(\omega_m)$, which tends to a finite value at $\omega_m \to 0$. At larger $\omega_m > \bar{g}$, both $\Delta_\infty(\omega_m)$ and $\Delta_0(\omega_m)$ scale as $1/|\omega_m|^2$. In Sec. III C, we obtain the solutions of the nonlinear gap equation in the order-by-order expansion in the gap magnitude and show that they form a one-parameter continuum set $\Delta_\xi(\omega)$, for which $\Delta_\infty(\omega_m)$ and $\Delta_0(\omega_m)$ are the two limiting cases. In Sec. IV, we analyze the properties of the gap function $\Delta(\omega)$ along the real frequency axis. We first obtain, in Sec. IV A, the exact solution of the linearized gap equation on the real axis, $\Delta_\infty(\omega)$, and show that it oscillates not only at $\omega < \bar{g}$, but also at $\omega > \bar{g}$, with a different period. In Sec. IV B, we consider the real-frequency form of $\Delta_0(\omega)$, which does not change sign on the Matsubara axis. We use as an input the results from earlier works [7–9], which demonstrated that $\Delta_0(\omega) = |\Delta_0(\omega)|e^{i\eta(\omega)}$ oscillates at $\omega > \bar{g}$, and argue that the phase $\eta(\omega)$ winds up by an infinite number of 2π between $\omega = O(\bar{g})$ and $\omega = \infty$. In Sec. IV C we present a one-parameter continuum set of $\Delta_\xi(\omega)$, which in the two limits reduces to $\Delta_\infty(\omega)$ and $\Delta_0(\omega)$. In Sec. V, we extend $\Delta_\xi(\omega)$ into the upper frequency half-plane ($\omega \to z$) and show that for each ξ, there is an infinite array of vortices in the upper frequency half-plane and an essential singularity at $|z| = \infty$. In Sec. VI, we consider the gap equation at a finite ω_D. We argue that the number of vortices becomes finite and the high-frequency behavior of the gap function becomes regular; however, this holds only above a frequency, which scales inversely with ω_D. In Sec. VII, we consider fluctuation corrections to superconducting order parameter $\Delta\langle e^{i\eta}\rangle$ We argue that the ground state is a superconductor, however corrections to $\langle e^{i\eta}\rangle$ become $O(1)$ already at $T \leqslant \omega_D$. We identify this scale with the actual superconducting T_c and discus pseudogap behavior in between $T_p \sim \bar{g}$ and T_c. In Sec. VIII, we combine the results for $\gamma = 2$ and for $\gamma < 2$ from papers I–IV and obtain the full phase diagram of the γ model for $\gamma \leqslant 2$. We present our conclusions in Sec. IX. Some technical aspects are discussed in Appendices.

II. ELIASHBERG EQUATIONS

The Eliashberg gap equation for the γ model is obtained by combining the equations for the pairing vertex Φ and the self-energy Σ. The two equations are obtained in a standard way, by summing up ladder series and neglecting vertex corrections (see paper I and the text below for justification). On the Matsubara axis, we have ($\Phi = \Phi(\omega_m)$, $\Sigma = \Sigma(\omega_m)$):

$$\Phi(\omega_m) = \bar{g}^\gamma \pi T \sum_{m'} \frac{\Phi(\omega_{m'})}{\sqrt{(\omega_{m'} + \Sigma(\omega_{m'}))^2 + \Phi^2(\omega_{m'})}} \frac{1}{\left(|\omega_m - \omega_{m'}|^2 + \omega_D^2\right)^{\gamma/2}},$$
$$\Sigma(\omega_m) = \bar{g}^\gamma \pi T \sum_{m'} \frac{\omega_{m'} + \Sigma(\omega_{m'})}{\sqrt{(\omega_{m'} + \Sigma(\omega_{m'}))^2 + \Phi^2(\omega_{m'})}} \frac{1}{\left(|\omega_m - \omega_{m'}|^2 + \omega_D^2\right)^{\gamma/2}}. \quad (1)$$

Introducing $\Delta(\omega_m) = \Phi(\omega_m)\omega_m/(\omega_m + \Sigma(\omega_m))$ and substituting into (1), we obtain after a simple algebra the equation that contains only $\Delta(\omega_m)$:

$$\Delta(\omega_m) = \bar{g}^\gamma \pi T \sum_{m'} \frac{\Delta(\omega_{m'}) - \Delta(\omega_m)\frac{\omega_{m'}}{\omega_m}}{\sqrt{(\omega_{m'})^2 + \Delta^2(\omega_{m'})}} \frac{1}{\left(|\omega_m - \omega_{m'}|^2 + \omega_D^2\right)^{\gamma/2}}. \quad (2)$$

For $\gamma = 2$, this reduces to

$$\Delta(\omega_m) = \bar{g}^2 \pi T \sum_{m'} \frac{\Delta(\omega_{m'}) - \Delta(\omega_m)\frac{\omega_{m'}}{\omega_m}}{\sqrt{(\omega_{m'})^2 + \Delta^2(\omega_{m'})}} \frac{1}{|\omega_m - \omega_{m'}|^2 + \omega_D^2}. \quad (3)$$

This is the same equation as for the interaction with an Einstein phonon [7–9,11–16,24,31–33]. As we said, we consider the limit $\omega_D \to 0$. The self-action term with $m' = m$ in the right-hand side (r.h.s.) of (3) can be safely eliminated because the numerator vanishes at $m = m'$. Setting then $\omega_D = 0$, we obtain the gap equation at a QCP:

$$\Delta(\omega_m) = \bar{g}^2 \pi T \sum_{m' \neq m} \frac{\Delta(\omega_{m'}) - \Delta(\omega_m)\frac{\omega_{m'}}{\omega_m}}{\sqrt{(\omega_{m'})^2 + \Delta^2(\omega_{m'})}} \frac{1}{(\omega_m - \omega_{m'})^2}. \quad (4)$$

At $T = 0$, $\pi T \sum_{m' \neq m} \to (1/2) \int d\omega'_m$.

The gap equation on the real axis is more conveniently expressed in terms of

$$D(\omega) = \Delta(\omega)/\omega. \tag{5}$$

The equation has the form [9]

$$D(\omega)\omega B(\omega) = A(\omega) + C(\omega), \tag{6}$$

where

$$\begin{aligned}
A(\omega) &= -\frac{\bar{g}^2}{2}\int_0^\infty d\omega' \Re \frac{D(\omega')}{\sqrt{1-D^2(\omega')}} A_T,\\
A_T &= \frac{\tanh\frac{\omega'}{2T}+\tanh\frac{\omega}{2T}}{(\omega'+\omega)^2} + \frac{\tanh\frac{\omega'}{2T}-\tanh\frac{\omega}{2T}}{(\omega'-\omega)^2} - \frac{1}{T\cosh^2\frac{\omega}{2T}}\,\frac{\omega'}{(\omega')^2-\omega^2},\\
B(\omega) &= 1 + \frac{\bar{g}^2}{2\omega}\int_0^\infty d\omega' \left[\Re\frac{1}{\sqrt{1-D^2(\omega')}}\right] B_T,\\
B_T &= \frac{\tanh\frac{\omega'}{2T}+\tanh\frac{\omega}{2T}}{(\omega'+\omega)^2} - \frac{\tanh\frac{\omega'}{2T}-\tanh\frac{\omega}{2T}}{(\omega'-\omega)^2} + \frac{1}{T\cosh^2\frac{\omega}{2T}}\,\frac{\omega}{(\omega')^2-\omega^2},\\
C(\omega) &= -i\frac{\bar{g}^2\pi}{2\sqrt{1-D^2(\omega)}}\left[\frac{dD(\omega)}{d\omega}\tanh\frac{\omega}{2T} - T\left(\frac{dD^2(\omega)}{d\omega^2} + \left(\frac{dD(\omega)}{d\omega}\right)^2\frac{D(\omega)}{1-D^2(\omega)}\right)\right],
\end{aligned} \tag{7}$$

where the integrals are principal values. At $T = 0$, the expressions simplify to

$$\begin{aligned}
A(\omega) &= -\bar{g}^2\int_0^\infty \frac{d\omega'}{(|\omega|+\omega')^2}\Re\frac{D(\omega')}{\sqrt{1-D^2(\omega')}},\\
B(\omega) &= 1 + \frac{\bar{g}^2}{|\omega|}\int_0^\infty \frac{d\omega'}{(|\omega|+\omega')^2}\Re\frac{1}{\sqrt{1-D^2(\omega')}},\\
C(\omega) &= -i\frac{\pi\bar{g}^2}{2\sqrt{1-D^2(\omega)}}\,\frac{dD(\omega)}{d\omega}\,\mathrm{sgn}\omega,
\end{aligned} \tag{8}$$

and the gap equation becomes

$$-i\frac{\pi\bar{g}^2}{2}\,\frac{\frac{dD(\omega)}{d\omega}}{\sqrt{1-D^2(\omega)}}\,\mathrm{sgn}\omega = D(\omega)\omega\left(1+\frac{\bar{g}^2}{|\omega|}\int_0^\infty\frac{d\omega'}{(|\omega|+\omega')^2}\Re\frac{1}{\sqrt{1-D^2(\omega')}}\right) + \int_0^\infty\frac{d\omega'}{(|\omega|+\omega')^2}\Re\frac{D(\omega')}{\sqrt{1-D^2(\omega')}}. \tag{9}$$

The functions $A(\omega)$ and $B(\omega)$ can be equivalently expressed in terms of the solution of the gap equation on the Matsubara axis [8,9,33]:

$$\begin{aligned}
A(\omega) &= 2\pi T\sum_{m=0}^{\infty}\frac{\Delta(\omega_m)}{\sqrt{\Omega_m^2+\Delta^2(\omega_m)}}\,\frac{\omega_m^2-\omega^2}{\left(\omega_m^2+\omega^2\right)^2},\\
B(\omega) &= 1 + 4\pi T\sum_{m=0}^{\infty}\frac{1}{\sqrt{\Omega_m^2+\Delta^2(\omega_m)}}\,\frac{\omega_m^2}{\left(\omega_m^2+\omega^2\right)^2}.
\end{aligned} \tag{10}$$

This simplifies numerical calculations: the recipe is to first solve for the gap at the Matsubata points $\omega_m = \pi T(2m+1)$ and then use Eqs. (10) as an input for the calculation of $D(\omega)$ on the real axis.

III. GAP EQUATION ALONG THE MATSUBARA AXIS AT $T = 0$

In papers I–IV, we analyzed the gap equation for $\gamma < 2$ and found that at $T = 0$ it has an infinite, discrete set of solutions at $\Delta(\omega_m) = \Delta_n(\omega_m)$. A gap function $\Delta_n(\omega_m)$ changes sign n times between $\omega_m = 0$ and $\omega_m = O(\bar{g})$ and decays as $1/|\omega_m|^\gamma$ at larger frequencies. The two end points of the set are the sign-preserving solution $\Delta_0(\omega_m)$ and the solution of the linearized gap equation $\Delta_\infty(\omega_m)$, which changes sign an infinite number of times. The existence of this infinite set is a distinct feature of the pairing at a QCP. Away from a QCP, the number of solutions becomes finite ($n = 0, 1\ldots, n_{\max}$), and far away from a QCP only the $n = 0$ solution remains, like in a conventional BCS/Eliashberg theory.

Here we extend this analysis to $\gamma = 2$. We show that for this γ, the set of gap functions becomes $\Delta_\xi(\omega_m)$, where $0 \leqslant \xi \leqslant \infty$ is a continuous variable. We first analyze the two end points, $\Delta_\infty(\omega_m)$ and $\Delta_0(\omega_m)$, and then obtain the gap function for arbitrary ξ.

A. Linearized gap equation

The linearized gap equation at $T = 0$ is obtained from (4) by assuming that the gap function is infinitesimally small, $\Delta(\omega_m) = \Delta_\infty(\omega_m)$. In terms of $D_\infty(\omega_m) = \Delta_\infty(\omega_m)/\omega_m$, we have

$$D_\infty(\omega_m) = \frac{\bar{g}^2}{2\omega_m}\int d\omega'_m \frac{D_\infty(\omega'_m) - D_\infty(\omega_m)}{(\omega_m - \omega_{m'})^2}\mathrm{sgn}\omega'_m. \quad (11)$$

One can verify that the leading term in $D_\infty(\omega_m)$ at small $\omega_m \ll \bar{g}$ is obtained by neglecting the l.h.s. of (11), i.e., by solving

$$\int_0^\infty d\omega'_m\left[\frac{D_\infty(\omega'_m) - D_\infty(\omega_m)}{(\omega_m - \omega_{m'})^2} + \frac{D_\infty(\omega'_m) + D_\infty(\omega_m)}{(\omega_m + \omega_{m'})^2}\right] = 0. \quad (12)$$

This approximation is equivalent to neglecting the bare ω in the fermionic propagator in comparison with the NFL fermionic self-energy without the self-action term, $\Sigma(\omega_m) = -\bar{g}^2/\omega_m$.

The solution of (12) is

$$D_\infty(\omega_m) = 2\epsilon\mathrm{Re}[e^{i(\beta\ln(\frac{|\omega_m|}{\bar{g}})^2+\phi)}]\mathrm{sgn}\omega$$
$$= 2\epsilon\cos\left(\beta\ln\left(\frac{|\omega_m|}{\bar{g}}\right)^2 + \phi\right)\mathrm{sgn}\omega, \quad (13)$$

where ϵ is an infinitesimally small real overall factor, ϕ is a phase factor, which is arbitrary at this stage, and $\beta = 0.38187$ satisfies $\pi\beta\tanh(\pi\beta) = 1$ and is the solution of

$$\int_{-\infty}^\infty dx\frac{|x|^{2i\beta} - \mathrm{sgn}x}{(x-1)^2} = 0, \quad (14)$$

The function $D_\infty(\omega_m)$ is scale-invariant (an arbitrary phase factor ϕ can be absorbed into the prefactor for ω under the logarithm). This is the consequence of the fact that $\bar{g}$ falls off from the gap equation (11), once we neglect $D_\infty(\omega_m)$ in the l.h.s.

We now analyze the full gap equation. By power counting, the r.h.s of (11) is of order $D_\infty(\omega_m)(\bar{g}/|\omega_m|)$. This justifies neglecting $D_\infty(\omega_m)$ in the l.h.s. for $|\omega_m| < O(\bar{g})$, but for larger frequencies it must be kept.

We obtained the exact solution of Eq. (11). The derivation parallels the one for smaller γ in papers I and IV. We skip the details and present the final result:

$$D_\infty(\omega_m) = \epsilon\frac{\bar{g}}{\omega_m}\int_{-\infty}^\infty dk b_k e^{-ik\ln(\omega_m/\bar{g})^2}, \quad (15)$$

where

$$b_k = \frac{e^{-iI_k}}{[\cosh(\pi(k-\beta))\cosh(\pi(k+\beta))]^{1/2}} \quad (16)$$

and

$$I_k = \frac{1}{2}\int_{-\infty}^\infty dk'\ln|\epsilon_{k'} - 1|\tanh\pi(k'-k+i\delta), \quad (17)$$

$$\epsilon_{k'} = \pi k'\tanh(\pi k'). \quad (18)$$

Here $\beta \simeq 0.38187$ is the same as in Eq. (13).

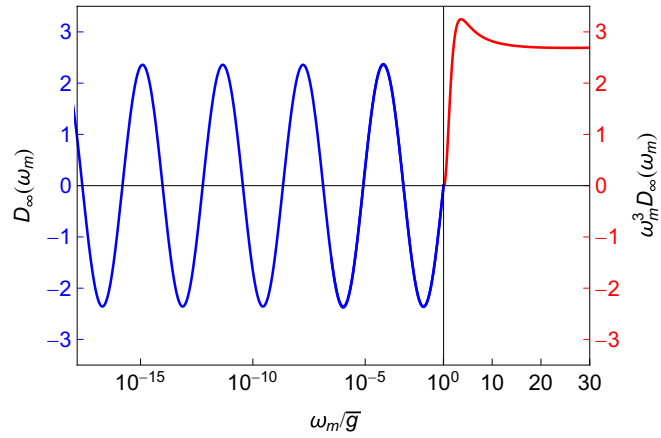

FIG. 1. $D_\infty(\omega_m)$ as a function of $\omega_m/\bar{g}$. The scale is logarithmic for $\omega_m < \bar{g}$ and linear at $\omega_m > \bar{g}$.

At $\omega_m \ll \bar{g}$, the exact $D_\infty(\omega_m)$ has the form of Eq. (13) with some particular ϕ. At $\omega_m \gg \bar{g}$, $D_\infty(\omega_m)$ does not oscillate and decreases as $1/(\omega_m)^3$ ($\Delta_\infty(\omega_m)$ decreases as $1/(\omega_m)^2$). We plot the exact $D_\infty(\omega_m)$ in Fig. 1. The crossover between the two forms occurs at $\omega_m \sim \bar{g}$, as expected.

The corrections to Eq. (13) at small ω_m hold in powers of $|\omega_m|/\bar{g}$; the leading correction scales as $(|\omega_m|/\bar{g})^{2.78}$. The corrections to $1/(\omega_m)^3$ at large ω_m hold in powers of $\bar{g}/|\omega_m|$; the leading correction scales as $(\bar{g}/|\omega_m|)^5\ln(|\omega_m|/\bar{g})$. We present the details of the analysis in Appendix B. There, we also show that at $\omega_m \gg \bar{g}$ there exists an exponentially small, oscillating component $D_{\infty;u}(\omega_m)$ in the form

$$D_{\infty;u}(\omega_m) \propto 2\sqrt{2}\epsilon e^{-(|\omega_m|/\bar{g})^2}\cos\left[\frac{(\pi^2-2)}{2\pi}\left(\frac{|\omega_m|}{\bar{g}}\right)^2 + \frac{\pi}{4}\right]. \quad (19)$$

This term is the contribution to D_∞ from large k and k' in Eqs. (16) and (17), It is completely irrelevant on the Matsubara axis, but we will see that it gives the dominant contribution to $D_\infty(\omega)$ on the real axis.

B. Nonlinear gap equation. Sign-preserving solution

We now analyze the full nonlinear gap equation, Eq. (4). We first search for a "conventional" sign-preserving solution $\Delta_0(\omega_m)$

The analytical analysis uses the same computational steps as in paper IV and we will be brief. We use the identity

$$\int_{-\infty}^\infty d\omega'_m\frac{1 - \frac{\omega'_m}{\omega_m}}{|\omega_m - \omega'_m|^\gamma} = 0, \quad (20)$$

valid for $\gamma > 1$, and re-express Eq. (4) as

$$\Delta_0(\omega_m)\left[1-\frac{\bar{g}^2}{2}\int_{-\infty}^{\infty}d\omega_m'\frac{1-\frac{\omega_m'}{\omega_m}}{|\omega_m-\omega_m'|^2}\left(\frac{1}{\sqrt{\Delta_0^2(\omega_m')+(\omega_m')^2}}-\frac{1}{\Delta_0(\omega_m)}\right)\right]=\frac{\bar{g}^2}{2}\int_{-\infty}^{\infty}d\omega_m'\frac{\Delta_0(\omega_m')-\Delta_0(\omega_m)}{|\omega_m-\omega_m'|^2\sqrt{\Delta_0^2(\omega_m')+(\omega_m')^2}}. \tag{21}$$

Both integrals in (21) are infra-red convergent and are determined by $\omega_m' \leqslant \Delta(\omega_m')$. In the limit $\omega_m \to 0$, Eq. (21) reduces to

$$\Delta_0(0)\left[1-\bar{g}^2\int_0^{\infty}d\omega_m'\frac{\sqrt{\Delta_0^2(\omega_m')+(\omega_m')^2}-\Delta_0(0)}{\Delta_0(0)\sqrt{\Delta_0^2(\omega_m')+(\omega_m')^2}|\omega_m'|^2}\right]=\bar{g}^2\int_0^{\infty}\frac{d\omega_m'\,(\Delta_0(\omega_m')-\Delta_0(0))}{\sqrt{\Delta_0^2(\omega_m')+(\omega_m')^2}|\omega_m'|^2}. \tag{22}$$

We assume and then verify that $\Delta_0(\omega_m') \approx \Delta_0(0)$ for $\omega_m' \leqslant \Delta_0(\omega_m')$, relevant for both integrals in (22). Substituting into (22), we find

$$1 \approx \bar{g}^2\int_0^{\infty}d\omega_m'\frac{\sqrt{\Delta_0^2(0)+(\omega_m')^2}-\Delta_0(0)}{\Delta_0(0)\sqrt{\Delta_0^2(0)+(\omega_m')^2}|\omega_m'|^2}. \tag{23}$$

The integral can be evaluated analytically and yields $\Delta_0(0) = \bar{g}$. Substituting further $\Delta_0(\omega_m') = \bar{g}$ into the r.h.s. of (21), we find that $\Delta_0(\omega_m)$ varies quadratically with ω_m at small ω_m and for $\omega_m \leqslant \bar{g}$ remains comparable to $\Delta_0(0)$. In the opposite limit of large ω_m, the prefactor for $\Delta_0(\omega)$ in the l.h.s. of (21) is approximately 1, and in the r.h.s. of this equation $1/|\omega_m|^2$ can be pulled out from the integral. This yields

$$\Delta_0(\omega_m) \approx Q\left(\frac{\bar{g}}{|\omega_m|}\right)^2, \tag{24}$$

where

$$Q=\int_0^{\infty}\frac{d\omega_m'\Delta_0(\omega_m')}{\sqrt{\Delta_0^2(\omega_m')+(\omega_m')^2}}. \tag{25}$$

The integral is determined by $\omega_m' \sim \bar{g}$ and is of order $\bar{g}$. Then $\Delta_0(\omega_m) \sim \bar{g}^3/|\omega_m|^2$ at high frequencies. The full gap function is sign-preserving. We show the numerical result for $\Delta_0(\omega_m)$ in Fig. 2. At small ω_m we find $\Delta_0(0) \approx 0.75\bar{g}$. This fully agrees with the earlier result, Ref. [8]. We note in passing that the first numerical evidence that $\Delta_0(0)$ scales with $\bar{g}$ has been obtained in Ref. [34].

C. Continuous set of solutions. Expansion in the gap magnitude

The solutions $\Delta_\infty(\omega_m)$ and $\Delta_0(\omega_m)$ (or, equivalently, $D_\infty(\omega_m)$ and $D_0(\omega_m)$) also exist for $\gamma < 2$. For such γ, these two solutions are the end points of a discrete set of topologically distinct solutions $\Delta_n(\omega)$. We argue below that the set becomes continuous for $\gamma = 2$. For a continuous set, there is no one-to-one correspondence between a particular member of the set and integer n, and we will show how this correspondence gets lost at $\gamma = 2 - 0$.

Comparing $D_\infty(\omega_m)$ and $D_0(\omega_m)$, we see that they have the same form $1/(\omega_m)^3$ for $\omega_m > \bar{g}$, but are very different for $\omega_m < \bar{g}$. We therefore focus on the range $\omega_m < \bar{g}$ and use to our advantage the fact that we know the analytic form of $D_\infty(\omega_m)$ in this range, Eq. (13). We use this $D_\infty(\omega_m)$ as an input and expand it in powers of $D^2(\omega_m')$ in the r.h.s. of the gap equation (4). Specifically, we will be searching for the solution of (4) in the form

$$D(\omega_m)=\sum_{j=0}^{\infty}D^{(2j+1)}(\omega_m), \tag{26}$$

where

$$D^{(1)}(\omega_m) = D_\infty(\omega_m) = 2\epsilon\cos f(\omega_m)\mathrm{sgn}\omega_m \tag{27}$$

with

$$f(\omega_m)=\beta\ln\left(\frac{|\omega_m|}{\bar{g}}\right)^2+\phi. \tag{28}$$

We will see that $D^{(2j+1)} \sim \epsilon^{2j+1}$.

Substituting $D(\omega_m)$ from (26) into (4) and expanding in $D^2(\omega_m')$ in the r.h.s. of (4), we obtain the set of equations, which express $D^{(2j+1)}$ for a given j in terms of $D^{(2j+1)}$ with smaller j. For $j = 1$, we have

$$D^{(3)}(\omega_m)\omega_m-\frac{\bar{g}^2}{2}\int d\omega_m'(D^{(3)}(\omega_m')-D^{(3)}(\omega_m))\times\frac{\mathrm{sgn}\omega_m'}{(\omega_m-\omega_m')^2}=K_3(\omega_m), \tag{29}$$

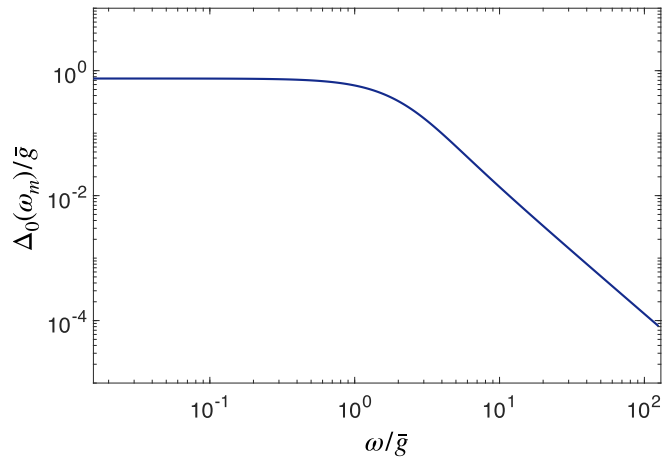

FIG. 2. Sign-preserving solution $\Delta_0(\omega_m)$ of the nonlinear gap equation along the Matsubara axis. We obtained $\Delta_0(\omega_m)$ by solving the nonlinear gap equation numerically and taking the limit $T \to 0$. At $\omega_m < \bar{g}$, $\Delta_0(\omega_m)$ remains comparable to $\bar{g}$; at larger frequencies it decays as $1/\omega_m^2$.

where the source term is

$$K_3(\omega_m) = -\frac{\bar{g}^2}{4}\int d\omega_m' (D^{(1)}(\omega_m') - D^{(1)}(\omega_m)) \times [D^{(1)}(\omega_m')]^2 \frac{\mathrm{sgn}\omega_m'}{(\omega_m - \omega_m')^2}. \quad (30)$$

The source term is of order ϵ^3, hence $D^{(3)} \propto \epsilon^3$ ($D^{(5)} \propto \epsilon^5$ and so on). Substituting $D^{(1)}(\omega_m)$ from Eq. (27) and evaluating the integrals, we find the source term for $D^{(3)}$ as the sum of the two terms, $K_3 = K_{3a} + K_{3b}$, where

$$K_{3a}(\omega_m) = -\epsilon^3 \frac{\bar{g}}{\omega_m} \cos(3f(\omega))(2\pi\beta\coth(2\pi\beta) - 3\pi\beta\tanh(3\pi\beta))\mathrm{sgn}\omega_m \quad (31)$$

and

$$K_{3b}(\omega_m) = -\epsilon^3 \frac{\bar{g}}{\omega_m} \cos(f(\omega)) \frac{1+\sinh^2(\pi\beta)}{\sinh^2(\pi\beta)} \mathrm{sgn}\omega_m. \quad (32)$$

Solving for $D^{(3)}$ we find that the first term gives rise to $\epsilon^3 \cos(3f(\omega))$, while the second term accounts for the renormalization of the prefactor for $\ln(\omega_m^2)$ in $f(\omega_m)$ in (28) To order ϵ^2, the dressed $f(\omega_m)$, which we label $f_\epsilon(\omega_m)$, becomes

$$f_\epsilon(\omega_m) = \beta_\epsilon \ln\left(\frac{|\omega_m|}{\bar{g}}\right)^2 + \phi_\epsilon, \quad (33)$$

where

$$\beta_\epsilon = \beta(1-\epsilon^2/2) \approx \beta(1-\epsilon^2)^{1/2}. \quad (34)$$

The full $D(\omega_m)$ to order ϵ^3 is

$$D(\omega_m) = 2(\epsilon\cos f_\epsilon(\omega_m) + Q_3\epsilon^3 \cos 3f(\omega_m))\mathrm{sgn}\omega_m, \quad (35)$$

where

$$Q_3 = \frac{2\pi\beta\coth(2\pi\beta) - 3\pi\beta\tanh(3\pi\beta)}{2(1-3\pi\beta\tanh(3\pi\beta))} = \frac{5-(\pi\beta)^2}{16} \approx 0.222. \quad (36)$$

Expanding to next order, we find (i) $\epsilon^5 \cos 5f(\omega_m)$ term with the prefactor $Q_5 = 0.043$, (ii) $O(\epsilon^4)$ corrections to β_ϵ in (34) [$\beta_\epsilon = 1 - 0.5\epsilon^2 + 0.806\epsilon^4$)], and (iii) $O(\epsilon^2)$ corrections to Q_3 ($Q_3 \to Q_{3,\epsilon}$) and to the argument of $\cos 3f(\omega_m)$ in (35). We verified that the last correction changes $\cos 3f(\omega_m)$ to $\cos 3f_\epsilon(\omega_m)$ with the same f_ϵ as in (33). This is the strong indication that the series contain the same fully renormalized $f_\epsilon(\omega_m)$ in each term. Combining the results, we obtain, for $\omega_m \ll \bar{g}$, $D(\omega_m) = D_\epsilon(\omega_m)$,

$$D_\epsilon(\omega_m) = 2\epsilon(\cos f_\epsilon(\omega_m) + Q_{3,\epsilon}\epsilon^3 \cos 3f_\epsilon(\omega_m) + Q_{5,\epsilon}\epsilon^5 \cos 5f_\epsilon(\omega_m) + \cdots)\mathrm{sgn}\omega_m. \quad (37)$$

We emphasize that a continuous set of solutions exists only for $\gamma = 2$. Applying the same perturbative analysis for $\gamma < 2$, we find that the expansion holds in $\epsilon^2(\bar{g}/|\omega_m|)^{2-\gamma}$ and breaks at a finite $\omega_{\min} \sim \bar{g}\epsilon^{2/(2-\gamma)}$ (see Appendix A for more detail). At smaller ω_m, $\Delta(\omega_m)$ saturates, and $D(\omega_m) \propto 1/\omega_m$. The forms of $D(\omega_m)$ at $\omega_m < \omega_{\min}$ and $\omega_m > \omega_{\min}$ match only for a discrete set of $\epsilon = \epsilon_n$, which implies that for $\gamma < 2$ the solutions of the full nonlinear gap equation form a discrete set.

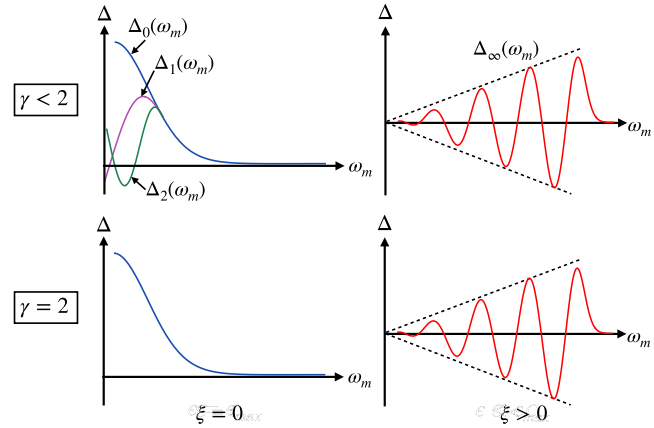

FIG. 3. The gap function $\Delta_n(\omega_m)$ for $\gamma<2$ and $\gamma=2$. For $\gamma < 2$, $\Delta_n(\omega_m)$ changes sign n times. As γ gets close to 2, the frequency region where these n sign changes happen, shrinks to progressively smaller $\omega_m = 0$, and at $\gamma = 2-0$, $\Delta_n(\omega_m)$ with finite n collapse into $\Delta_0(\omega_m)$ at all $\omega_m > 0$. The continuum set of $\Delta_\xi(\omega_m)$ at $\gamma = 2-0$ emerges from $\Delta_n(\omega_m)$ with $n \to \infty$, and the continuous parameter ξ is determined by how the double limit $n \to \infty$ and $\gamma \to 2$ is taken. As the consequence, all $\Delta_\xi(\omega_m)$ with $\xi > 0$ change sign infinite number of times between $\omega_m = 0$ and $\omega_m \sim \bar{g}$. The solution of the linearized gap equation is the $\xi \to \infty$ limit of this set.

Because $f_\epsilon(\omega_m)$ contains $\ln\omega_m^2$, each $D_\epsilon(\omega_m)$ from (37) changes sign an infinite number of times down to $\omega_m = 0$, i.e., in our original classification the gap functions from the set are different realizations of $n = \infty$. At $\omega_m = 0$, each $D_\epsilon(\omega_m)$ has an essential singularity as neither $\lim_{\omega_m\to 0} D_\epsilon(\omega_m)$ nor $\lim_{\omega_m\to 0} 1/D_\epsilon(\omega_m)$ exist.

For a generic ϵ, Eq. (37) is valid for $\omega_m < \bar{g}$. At larger ω_m, $D_\epsilon(\omega_m) = D_\epsilon/|\omega_m|^2$. We expect that for every ϵ, the crossover to proper high-frequency behavior can be achieved by fixing the phase factor ϕ_ϵ in (33) (see paper I for a similar analysis for the linearized gap equation for $\gamma < 1$).

Next, we see from Eq. (34) that β_ϵ^2 decreases with increasing ϵ. It is natural to expect that it vanishes at some $\epsilon_{cr} = O(1)$. The expansion in (37) holds only as long as β_ϵ is real, as there is no solution of the non-linear gap equation for imaginary β_ϵ (see paper I for detailed discussion on this). For $\epsilon \leqslant \epsilon_{cr}$, β_ϵ is small, and the range, where $D(\omega_m)$ oscillates, is confined to small $\omega_m \leqslant \bar{g}e^{-\pi/\beta_\epsilon}$. By properly taking the double limit $\epsilon \to \epsilon_{cr}$ and $\omega_m \to 0$, one can obtain an infinite set of gap functions, which change sign a given number of times in the immediate vicinity of $\omega_m = 0$. At $\epsilon = \epsilon_{cr}$ all these gap functions coincide with $\Delta_0(\omega_m)$ at any $\omega_m > 0$. This agrees with the observation in paper IV that as γ increases towards 2, the region, where $\Delta_n(\omega_m)$ with finite n change sign, gets confined to progressively smaller ω_m, while at larger ω_m, all $\Delta_n(\omega_m)$ with $n = 0, 1, 2\ldots$ nearly coincide. We illustrate this in Fig. 3. For consistency with the notations in previous sections, it is convenient to introduce $\xi = (\epsilon_{cr} - \epsilon)/\epsilon$ and label the continuum set of the gap functions by $\Delta_\xi(\omega_m)$. Then the end point solutions $\epsilon \to 0$ and $\epsilon = \epsilon_{cr}$ are $\Delta_\infty(\omega_m)$ and $\Delta_0(\omega_m)$.

It is beyond the ability of the order-by-order expansion to determine the form of $\Delta_\xi(\omega_m)$ near $\xi = 0$. On general grounds, we expect that corrections to $f_\epsilon(\omega_m) \to f_\xi(\omega_m)$ in (33) become relevant starting already from small frequencies, and that at $\xi = 0$, the gap function coincides with $\Delta_0(\omega_m)$, which we found in the previous section. A way to reproduce this behavior is to assume that at $\xi \to 0$, the series for $D(\omega_m)$ in (37) become geometrical [$Q_{2n+1}\epsilon_{\rm cr}^{2n+1} \approx (-1)^n$]. In this case,

$$D_\xi(\omega_m) \sim \frac{\cos f_\xi(\omega_m)}{\alpha^2 + \cos^2 f_\xi(\omega_m)} \mathrm{sgn}\omega_m, \tag{38}$$

where $\alpha \sim \xi^2$ and $f_\xi(\omega_m) \sim \sqrt{\alpha}\ln \bar{g}/|\omega_m| + f^*(\omega_m)$, where $f^*(\omega_m)$ is a regular function of ω_m, which at low frequencies reduces to $\pi/2 + O(\omega_m/\bar{g})$. For any $\xi > 0$, this $D_\xi(\omega_m)$ changes sign an infinite number of times, but at $\xi = 0$, $D_{\xi=0}(\omega_m) \sim \bar{g}/\omega_m$, as we expect. We also note that between the nodes (the vortex points), $D_\xi(\omega_m)$ from (38) is large, of order $1/\xi$. Extending this $D(\omega_m)$ to complex frequencies, $z = \omega' + i\omega''$, we find that there exist antivortices at small z in the lower frequency half-plane. At $\xi = 0$, vortices and antivortices annihilate at $z = 0$, leaving a regular gap function $\Delta_0(\omega_m)$.

In Appendix C, we consider the extended $\gamma-$ model with nonequal interactions in the particle-particle and particle-hole channels and introduce $M \neq 1$ as a measure of the difference of the two interactions. For the extended model, there is a critical $M_{\rm max}$, below which the ground state is a non-Fermi liquid with $\Delta = 0$. For $\gamma = 2$, $M_{\rm max} = 0$. We obtain the set of $\Delta_\xi(\omega_m)$ at small ω_m at $M = 0+$ and show that all gap functions from the continuous set appear simultaneously with the overall magnitude $M^{1/2}$.

We next analyze the condensation energy E_c. We define E_c as the difference between the actual ground state energy E_Δ at a finite $\Delta(\omega_m)$ and the would be ground state energy of the normal state, $E_{\Delta=0}$. The expression for E_c for $\gamma = 2$ has been obtained before [32,35–37] and we just copy it here:

$$\begin{aligned} E_c = &-N_0 \int_0^\infty d\omega_m \omega_m \frac{(\sqrt{1+D^2(\omega_m)} - 1)^2}{\sqrt{1+D^2(\omega_m)}} \\ &- N_0 \bar{g}^2 \int_0^\infty d\omega_m d\omega'_m \frac{(\sqrt{1+D^2(\omega_m)} - \sqrt{1+D^2(\omega'_m)})^2}{\sqrt{1+D^2(\omega_m)}\sqrt{1+D^2(\omega'_m)}} \\ &\times \frac{\omega_m \omega'_m}{\left(\omega_m^2 - (\omega'_m)^2\right)^2}. \end{aligned} \tag{39}$$

This formula has been derived with the use of (4) and is therefore valid only for the solutions of the gap equation. Both terms in (39) are negative, i.e., any solution of the gap equation lowers the ground state energy compared to the normal state.

Substituting (37) into (39), we find that $E_c = E_{c,\xi}$ is a continuous function of ξ. At $\xi \gg 1$,

$$E_{c,\xi} = -aN_0 \frac{\bar{g}^2}{\xi^4}, \tag{40}$$

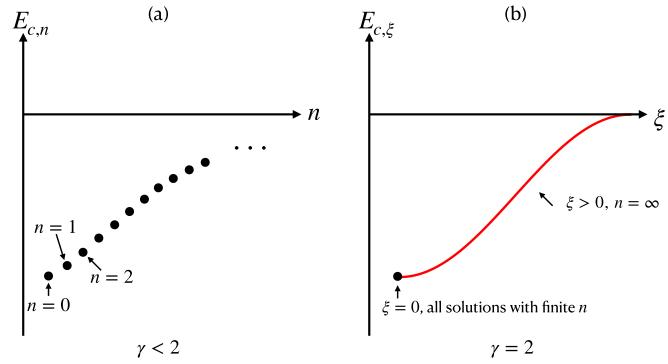

FIG. 4. (a) The condensation energy E_c the solutions of the Eliashberg gap equation for $\gamma < 2$. $E_c = E_{c,n}$ is a discrete function of a number of a solution, n. The largest condensation energy is for $n = 0$. (b) The condensation energy $E_{c,\xi}$ for $\gamma = 2$. $E_{c,\xi}$ is a continuous function of the parameter ξ. The condensation energy at $\xi = 0$ is the accumulation point of all $E_{c,n}$ from $\gamma < 2$ with finite $n = 0, 1, \ldots$ Every other point on the curve $E_{c,\xi}$ comes from the limit $n \to \infty$, and different ξ correspond to different ways how the double limit $n \to \infty$ and $\gamma \to 2$ is taken. In the limit $\xi \to \infty$, E_c is the condensation energy for infinitesimally small gap function $\Delta_\infty(\omega_m)$.

where $a = O(1)$. It is natural to expect that $|E_{c,\xi}|$ increases with decreasing ξ and reaches a maximum at $\xi = 0$, see Fig. 4.[3]

In the next two sections, we present corroborative evidence for the special, critical behavior of the γ model with $\gamma = 2$ from the analysis of the gap function on the real frequency axis and in the upper half-plane of frequency.

IV. GAP EQUATION ALONG THE REAL FREQUENCY AXIS

As we said in Introduction, the analysis of the gap equation for the γ model along real frequency axis should generally be more revealing than the analysis along the Matsubara axis, because the pairing interaction on the real axis $V(\Omega) = (\cos(\pi\gamma/2) + i\mathrm{sgn}(\Omega)\sin(\pi\gamma/2))(\bar{g}/|\Omega|)^\gamma$ is complex. The real part of the interaction becomes repulsive for $\gamma > 1$, and the imaginary part vanishes at $\gamma = 2$ for any nonzero Ω. This makes the $\gamma = 2$ case special.

We present the results for $\Delta(\omega)$ on the real axis in the same order as in previous section: we first obtain the solution of the linearized gap equation, which we label $\Delta_\infty(\omega)$, then analyze the solution $\Delta_0(\omega)$, and then show that there is a one-parameter continuous set of solutions $\Delta_\epsilon(\omega)$ in between $\Delta_\infty(\omega)$ and $\Delta_0(\omega)$.

A. Linearized gap equation in real frequencies

The linearized gap equation in real frequencies is obtained by taking the limit $\Delta(\omega) \to 0$ in (9). We again introduce

[3]The second term in (39) diverges logarithmically at $\xi = 0$ if we use $D_0(\omega) \approx \Delta(0)/\omega$ at small frequencies. This divergence comes from the putative normal state energy $E_{\Delta=0}$ while the ground state energy E_Δ remains finite. For $\xi > 0$, both $E_{\Delta=0}$ and E_Δ have logarithmic singularities, which cancel out in $E_c = E_\Delta - E_{\Delta=0}$.

$D_\infty(\omega) = \Delta_\infty(\omega)/\omega$ and re-write the gap equation as

$$D_\infty(\omega) = -\frac{\bar{g}^2}{\omega}\left[i\frac{\pi}{2}\frac{dD_\infty(\omega)}{d\omega}\mathrm{sgn}\omega + \frac{D_\infty(\omega)}{\omega} + \int_0^\infty \frac{d\omega'}{(|\omega|+\omega')^2}\,\Re D_\infty(\omega')\right], \quad (41)$$

where $\Re$ stands for the real part. The $D_\infty(\omega)$ term in the l.h.s. of (41) is the analog of $D_\infty(\omega_m)$ in the l.h.s. of the gap equation (11) on the Matsubara axis, and, like there, it originates from the bare ω term in the fermionic Green's function. Neglecting this term, we find that the solution of (41) is

$$D_\infty(\omega) = -2i\epsilon\cos\left[\beta\left(\ln\left(\frac{\omega}{\bar{g}}\right)^2 - i\pi\,\mathrm{sgn}(\omega)\right) + \phi\right], \quad (42)$$

where $\beta = 0.38187$ the same as in (13), and ϵ is infinitesimally small. We note that this $D_\infty(\omega)$ can be obtained from $D_\infty(\omega_m)$, Eq. (13), by rotating from $i\omega_m$ to $\omega + i0$. In explicit form,

$$D'_\infty(\omega) = 2\epsilon\sin\left(\beta\ln\left(\frac{\omega}{\bar{g}}\right)^2 + \phi\right)\sinh(\pi\beta)\mathrm{sgn}\omega,$$

$$D''_\infty(\omega) = -2\epsilon\cos\left(\beta\ln\left(\frac{\omega}{\bar{g}}\right)^2 + \phi\right)\cosh(\pi\beta). \quad (43)$$

Observe that $D'_\infty(-\omega) = -D'_\infty(\omega)$ and $D''_\infty(-\omega) = D''_\infty(\omega)$, as it should be. The relation

$$\int_0^\infty dx\,\frac{x^{2i\beta}}{(x+1)^2} = \frac{2\pi\beta}{\sinh(2\pi\beta)} = \frac{1}{\sinh^2(\pi\beta)}, \quad (44)$$

is useful for the verification that $D_\infty(\omega)$ satisfies Eq. (41) without $D_\infty(\omega)$ in the l.h.s. Using another relation

$$\int_0^\infty dx\,\frac{x^{i\beta}}{x-1} = i\pi\coth(\pi\beta), \quad (45)$$

one can verify that D'_∞ and D''_∞ satisfy KK relations:

$$\frac{2}{\pi}\int dx\frac{D'_\infty(x)x}{x^2-\omega^2} = -D''_\infty(\omega), \quad \frac{2\omega}{\pi}\int dx\frac{D''_\infty(x)}{x^2-\omega^2} = D'_\infty(\omega), \quad (46)$$

where the integrals are principle values.

We next consider $|\omega| > \bar{g}$. To obtain $D_\infty(\omega)$ in this region, we take as an input the exact solution on the Matsubara axis and analytically continue it to the real axis. By construction, this can be done by replacing ω_m by $(-iz)$—the function $\Delta_\infty(z)$ is guaranteed to be analytic in the upper half-plane of frequency. However, because we don't have the exact analytical expression for $D_\infty(\omega_m)$ for an arbitrary ω_m, we have to replace ω_m by $-i(\omega + i0)$ in Eq. (15) and obtain $\Delta_\infty(\omega)$ by integrating over k. For small $\omega < \bar{g}$, we find, after this integration, series of corrections to (42) in powers of $\omega/\bar{g}$. For large $\omega > \bar{g}$, the largest contribution to $\Delta_\infty(\omega)$ comes from the continuation of the universal oscillating term $\Delta_{\infty;u}$, Eq. (19). Upon rotation to the real axis, this term splits into two. One remains exponentially small, but in the other the exponential factor cancels out. As a result, on the real axis we have (see Appendix B for details)

$$D_{\infty;u}(\omega) \sim \sqrt{2}\epsilon e^{\frac{i}{\pi}\left[\left(\frac{\omega}{\bar{g}}\right)^2 + \ln\left(\frac{\omega}{\bar{g}}\right)^2\right]}. \quad (47)$$

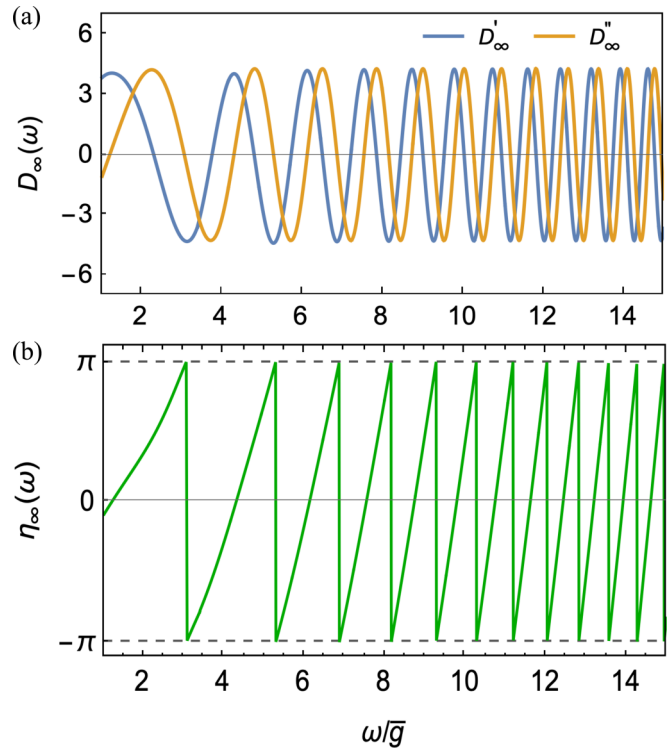

FIG. 5. Real and imaginary parts (a) and the phase $\eta_\infty(\omega)$ (b) of $D_\infty(\omega)$. The periodicity of oscillation is set by $[(\omega/\bar{g})^2 + \ln(\omega/\bar{g})^2]/\pi$.

Other contributions contain powers of $\bar{g}/|\omega|$ and are smaller. Neglecting them, we obtain $D_\infty(\omega) = D_{\infty;u}(\omega)$ at $\omega \gg \bar{g}$.

Comparing this form with (42), we see that both $D'_\infty(\omega)$ and $D''_\infty(\omega)$ continue oscillating at $\omega > \bar{g}$, but with the period set predominantly by $(\omega/\bar{g})^2$ rather than by $\ln(\omega/\bar{g})^2$. In Fig. 5, we plot real and imaginary parts of $D_\infty(\omega)$ and the phase of the gap, $\eta_\infty(\omega)$, defined via $D_\infty(\omega) = |D_\infty(\omega)|e^{i\eta_\infty(\omega)}$, or, equivalently, via $\eta_\infty(\omega) = \mathrm{Im}\ln D_\infty(\omega) = \mathrm{Im}\ln\Delta_\infty(\omega)$. We see that the phase winds up an infinite number of times between $\omega = 0$ and $O(\bar{g})$ and between $O(\bar{g})$ and ∞. Oscillations at $\omega < \bar{g}$ are directly related to oscillations of $\Delta_\infty(\omega_m)$ on the Matsubara axis, and there is one-to-one correspondence between each phase winding by 2π on a real axis and a vortex on the Matsubara axis. Oscillations and phase winding at $\omega > \bar{g}$ are present on the real axis, but not on the Matsubara axis. It is natural to relate this discrepancy to the fact that the pairing interaction is attractive on the Matsubara axis, but on the real axis, $V'(\Omega)$ is repulsive, and a nonzero $D_\infty(\omega)$ comes from $V''(\Omega) \propto \delta(\Omega^2)$ (see more on this below).

B. The function $D_0(\omega)$

We now consider the opposite limit of the real-axis partner of sign-preserving $D_0(\omega_m)$. At $\omega_m < \bar{g}$, $D_0(\omega_m) \approx \Delta_0(0)/\omega_m$, and $D_0(\omega)$ on the real axis must also be close to $D_0(0)/\omega$ at $\omega < \bar{g}$. At larger $\omega_m > \bar{g}$, we will see that $D_0(\omega_m)$ and $D_0(\omega)$ are very different: $D_0(\omega_m)$ decays as $1/\omega_m^3$, while $D_0(\omega)$ does not decay and oscillates in sign.

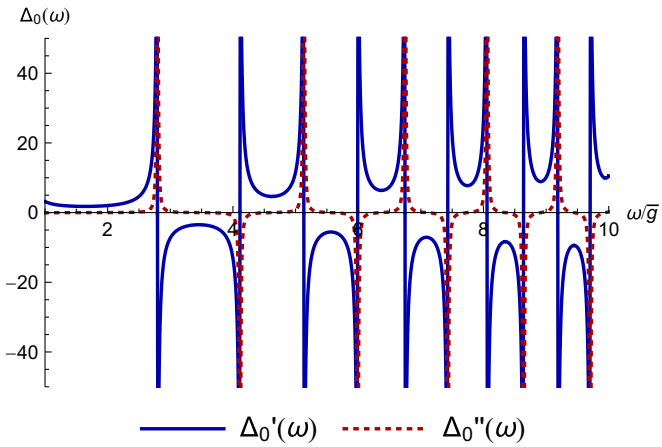

FIG. 6. $\Delta_0(\omega) = \omega/\sin\phi_0(\omega)$ for $\phi_0(\omega)$ given by (49). The real part of the gap $\Delta_0'(\omega)$ diverges at the set of points where $\phi_0(\omega) = p\pi$, $p = 1, 2\ldots$ The imaginary part $\Delta_0''(\omega)$ is a set of δ functions at these points. The behavior of $\Delta_0'(\omega)$ has been obtained in Refs. [7–9,11].

The solution of the gap equation along the real axis for $\omega > \bar{g}$ has been found by Combescot [9], who build his analysis on earlier results by Karakozov, Maksimov, and Mikhailovsky [7] and by Marsiglio and Carbotte [8]. We follow Ref. [9] below.

It is convenient to introduce $\phi_0(\omega)$ via $D_0(\omega) = 1/\sin\phi_0(\omega)$ and re-express the gap equation (9) at $T = 0$ as the equation on $\phi(\omega)$. The equation is

$$\frac{d\phi_0(\omega)}{d\omega} = \frac{2}{\pi\bar{g}^2}[\omega B(\omega) - A(\omega)\sin\phi_0], \tag{48}$$

where $A(\omega)$ and $B(\omega)$ are given by Eq. (8). The initial condition for ϕ_0 is $\phi_0(\bar{g}) \approx \bar{g}/\Delta_0(0) = O(1)$, consistent with $\phi_0(\omega) \approx \omega/\Delta_0(0)$ at $\omega < \bar{g}$.

At $\omega \gtrsim \bar{g}$, $B(\omega) \approx 1 + \bar{g}^2/\omega^2$ and $A(\omega) \approx -\alpha\bar{g}^3/\omega^2$, where $\alpha \approx 1.27$ (Ref. [9]). The $A(\omega)$ term can then be neglected if $\phi_0(\omega)$ is real, as we will assume and then verify. Without this term, Eq. (48) can be solved easily, and the result is

$$\phi_0(\omega) \approx \frac{1}{\pi}\left(\ln\left(\frac{\omega}{\bar{g}}\right)^2 + \left(\frac{\omega}{\bar{g}}\right)^2 + C\right), \tag{49}$$

where $C = \bar{g}/\Delta_0(0) - 1/\pi$. We see that $\phi_0(\omega)$ is real, as we anticipated. We note that this $\phi_0(\omega)$ coincides with the argument of the exponent for $D_\infty(\omega)$ in (47)

The function

$$D_0(\omega) = \frac{1}{\sin\phi_0(\omega + i0)} \tag{50}$$

is a sign-changing function of ω, whose real part almost diverges at a set of frequencies where $\phi_0(\omega) = p\pi$, and $p = 1, 2\ldots$ is an integer. The imaginary component $D_0''(\omega)$ is a set of δ functions at these frequencies. We plot the gap function $\Delta_0(\omega) = \omega D_0(\omega)$ in Fig. 6.

To analyze the phase winding, we again introduce the phase factor via $D_0(\omega) = |D_0(\omega)|e^{i\eta_0(\omega)}$ and consider how $\eta_0(\omega)$ varies at $\omega \gtrsim \bar{g}$. The imaginary component $D_0''(\omega)$ in (50) is infinitesimally small, except in the vicinity of ω_p, where $\phi_0(\omega_p) = p\pi$. We use Eq. (49) for $\phi_0(\omega)$ and express

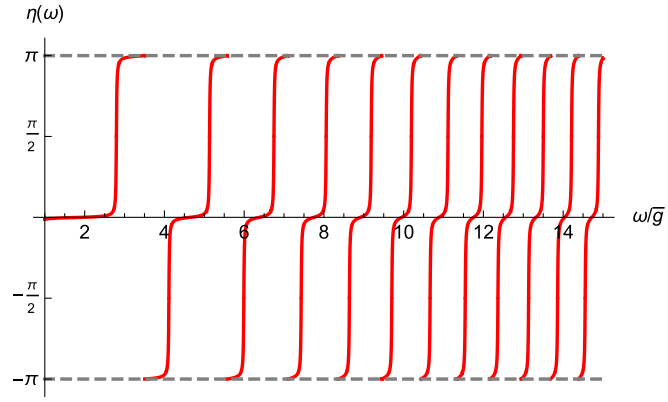

FIG. 7. Variation of the phase of the gap $\eta_0(\omega)$ ($\Delta_0(\omega) = |\Delta_0(\omega)|e^{i\eta_0(\omega)}$). We restrict $\eta_0(\omega)$ to $(-\pi, \pi)$. Phase slips of $\eta_0(\omega)$ continue up to infinite frequency.

$D_0(\omega)$ near each such point as

$$D_0(\omega) \approx \frac{\pi\bar{g}^2}{2}\frac{(-1)^p\omega_p}{\omega_p^2 + \bar{g}^2}\frac{1}{\omega - \omega_p + i\delta}. \tag{51}$$

Then

$$e^{i\eta_0(\omega)} = (-1)^p\frac{\omega - \omega_p - i\delta}{\sqrt{(\omega - \omega_p)^2 + \delta^2}}. \tag{52}$$

We plot $\eta_0(\omega)$ in Fig. 7. We see that the phase rapidly changes by π around each ω_p. If we restrict $\eta_0(\omega)$ to $(-\pi, \pi)$, we find that the phase jumps by 2π in between ω_p and ω_{p+1}. The number of ω_p is infinite, hence the number 2π jumps is also infinite. We reiterate that behavior has no analog the Matsubara axis, where $D_0(i\omega_m)$ is real and positive for $\omega_m > 0$, hence $\eta_0 = 0$.[4]

C. The one-parameter set of gap functions

We follow the same strategy as in the analysis on the Matsubara axis and expand the nonlinear gap equation (9) in powers of D^2. We search for the solution in the form

$$D(\omega) = \sum_{j=0}^{\infty} D^{(2j+1)}(\omega), \tag{53}$$

where $D^{(1)}(\omega) = D_\infty(\omega)$ and higher-order terms are obtained by solving Eq. (9) iteratively. For $\omega < \bar{g}$, we use Eq. (42) for $D_\infty(\omega)$. The computational steps are the same as in Sec. III C, and we obtain

$$D_\epsilon(\omega) = -2i\epsilon(\cos\tilde{f}_\epsilon(\omega) + \epsilon^2 Q_{3,\epsilon}\cos 3\tilde{f}_\epsilon(\omega) + \epsilon^4 Q_{5,\epsilon}\cos 5\tilde{f}_\epsilon(\omega) + \ldots), \tag{54}$$

[4]For a generic γ, $\Delta_0(\omega_m)$ and $\Delta_0''(\omega)$ are related by Cauchy formula: $\Delta_0(\omega_m) = (2/\pi)\int_0^\infty d\omega\Delta_0''(\omega)\omega/(\omega^2 + \omega_m^2)$. For $\gamma < 2$, typical ω are of order ω_m, and to reproduce $\Delta_0(\omega_m) \propto 1/|\omega_m|^\gamma$ one needs $\Delta_0''(\omega) = \sin(\pi\gamma/2)\,\mathrm{sgn}\omega/|\omega|^\gamma$. The case $\gamma = 2$ is an exception here because $1/\omega_m^2$ dependence of $\Delta_0(\omega_m)$ is obtained by pulling $1/\omega_m^2$ out of the denominator in the Cauchy formula. The remaining integral is determined by $\omega = O(\bar{g})$ rather than $O(\omega_m)$. Because of this, the fact that $\Delta_0(\omega_m) \propto 1/\omega_m^2$ at large frequencies does not imply that $\Delta''(\omega)$ must behave as $1/\omega^2$.

where $Q_{i,\epsilon}$ are the same as in (37) and

$$\tilde{f}_\epsilon(\omega) = \beta_\epsilon\left(\ln\left(\frac{\omega}{\bar{g}}\right)^2 - i\pi\,\mathrm{sgn}\omega\right) + \phi_\epsilon. \tag{55}$$

This $D_\epsilon(\omega)$ could also be obtained directly from (37) by replacing $\ln\omega_m^2$ by $\ln\omega^2 - i\pi$ in each term in (37).

We recall that the continuous set exists for $\epsilon \leqslant \epsilon_{\rm cr}$. For any $\epsilon < \epsilon_{\rm cr}$, $D(\omega)$ oscillates an infinite number of times down to $\omega = 0$. As ϵ approaches $\epsilon_{\rm cr}$, log-oscillations shift to progressively smaller frequencies. At $\epsilon = \epsilon_{\rm cr}$, β_ϵ vanishes and log-oscillations disappear. The behavior of $D(\omega)$ at $\omega \to 0$ at $\epsilon \to \epsilon_{\rm cr}$ depends on how the double limit $\omega \to 0$ and $\epsilon \to \epsilon_{\rm cr}$ is taken.

Like we did in Sec. III C, we introduce $\xi = (\epsilon_{\rm cr} - \epsilon)/\epsilon$ and re-express $\Delta_\epsilon(\omega)$ as $\Delta_\xi(\omega)$. The two limits $\epsilon = 0$ and $\epsilon = \epsilon_{\rm cr}$ now correspond to $\xi = \infty$ and $\xi = 0$, respectively. This brings the notations in line with the ones we used in Secs. IV A and IV B.

On the Matsubara frequency, all $\Delta_\xi(\omega_m)$ behave in the same way at $\omega_m > \bar{g}$: $\Delta_\xi \propto 1/\omega_m^2$. On the real axis, the dependence on ξ is more complex. To see this, we use the solution of the linearized gap equation $D^{(1)} \propto ie^{i\phi_0(\omega)}$ with $\phi_0(\omega)$, given by (49), and evaluate $D^{(2n+1)}$ in order-by-order expansion of the nonliner gap equation in D^2. Collecting the series, we obtain the closed form expression

$$\begin{aligned} D_\xi(\omega) &= \frac{-2ie^{i\phi_0(\omega)}}{1+\xi - e^{2i\phi_0(\omega)}/(1+\xi)} \\ &= \frac{1}{\sin[\phi_0(\omega) + i\ln(1+\xi)]}. \end{aligned} \tag{56}$$

This expression can be equivalently obtained by solving Eq. (48) for $\phi(\omega)$ with the initial condition $\phi(\bar{g}) = \bar{g}/\Delta_0(0) + i\ln(1+\xi)$.

The parameter ξ runs between 0 and ∞. For $\xi = 0$, Eq. (56) yields $D_0(\omega) = 1/\sin\phi_0(\omega)$, which agrees with (50) (one should add $i0$ to ω in this case). At $\xi \to \infty$, we recover, by construction, the solution of the linearized gap equation. For any ξ, including $\xi = 0$, $D_\xi(\omega)$ oscillates up to an infinite frequency, and its phase $\eta_\xi(\omega)$ winds up by an infinite number of 2π between $\omega \sim \bar{g}$ and $\omega = \infty$.

We see therefore that in both limits $\omega \ll \bar{g}$ and $\omega \gg \bar{g}$, the solutions of the nonlinear gap equation form a continuous one-parameter set, Eqs. (54) and (56). We conjecture that for any value of ξ, one can use a free phase factor ϕ_ξ in (55) to merge small-ω and large-ω expressions into a single $D_\xi(\omega)$.

D. Density of states

The fermionic DoS is defined as $N(\omega) = (-N_0/\pi)\mathrm{Im}G_l(\omega)$, where N_0 is the DoS in the normal state and

$$G_l(\omega) = -i\pi\sqrt{\frac{1}{1-D^2(\omega)}} \tag{57}$$

is a retarded Green's function, integrated over the dispersion.

In a BCS superconductor, $N(\omega) \propto \mathrm{Re}\omega/\sqrt{\omega^2 - \Delta^2}$ vanishes at $\omega < \Delta$, has an integrable singularity at $\omega = \Delta + 0$, and is nonzero for all $\omega > \Delta$ because quasiparticle states in a BCS superconductor form a continuum $\omega = \pm\sqrt{\Delta^2 + (\epsilon_k - \mu)^2}$. In our case, the form of $N(\omega) = N_\xi(\omega)$ strongly depends on ξ. At small $\omega < \bar{g}$, $N_\xi(\omega)$ remains finite down to $\omega = 0$ for all $\xi > 0$. In this respect, all such solutions describe gapless superconductivity. The gap function $\Delta_0(\omega)$ tends to a finite $\Delta_0(0)$ at small ω, and the corresponding $N_0(\omega)$ vanishes, like in BCS superconductor. We show this in Fig. 8(a).

At $\omega > \bar{g}$, $\Delta_\xi(\omega)$ is given by (56), and $N_\xi(\omega) = N_0\Im\tan[\phi_0(\omega) + i\ln(1+\xi)]$. For $\xi > 0$, $N_\xi(\omega)$ oscillates around N_0 up to $\omega = \infty$. The amplitude of the oscillations increases with decreasing ξ. For $\xi = 0$, $N_0(\omega) = N_0\delta/(\cos^2\phi_0(\omega) + \delta^2)$, where $\delta = 0+$. This DoS consists of a set of δ functions at the points ω_k, for which $\phi_0(\omega_k) = \pi/2 + k\pi$ (k is an integer) (Refs. [9,11,12]). We show this in Fig. 8(b). In Fig. 8(c) we show $N_\xi(\omega)$ in the whole range of frequencies.

The function $N_0(\omega)$ is the true DoS at $T = 0$, as the $\xi = 0$ solution has the lowest condensation energy. It is different from the DoS in a BCS-type superconductor, which is nonzero at all $\omega > \Delta$ and approaches N_0 at $\omega \to \infty$. We emphasize that a qualitative distinction holds only for $\gamma = 2$. For smaller γ, the DoS for the $n = 0$ solution evolves as a function of frequency, but still remains nonzero at all $\omega > \Delta$ and approaches N_0 at infinite ω (see paper IV).

In a BCS superconductor, a continuous $N(\omega)$ at $\omega > \Delta$ is the consequence of the fact that fermionic energy E_k is a continuous function of the normal state dispersion ϵ_k, $E_k = \sqrt{\epsilon_k^2 + \Delta^2}$. The form of $N_0(\omega)$ as a set of δ-functional peaks raises the issue whether fermionic energies get quantized at $\gamma = 2$. To address this issue, we compute the total weight of each level: $N_k = (1/2\pi)\int N_0(\omega)/N_0$, where the integration is confined to the vicinity of ω_k. Using $\phi_0(\omega) \approx \omega^2/\pi$, we obtain $N_k = 1/\sqrt{8(1+2k)}$. We see that $N_k < 1$ for all k. Because of this, ω_k cannot be viewed as true quantized fermionic energy levels, as a fermion is necessary distributed between ω_k with different k.

V. GAP FUNCTION IN THE UPPER FREQUENCY HALF-PLANE

Comparing $D_\xi(\omega)$ and $D_\xi(\omega_m)$, we see that they are similar at small frequencies, but very different at $\omega, \omega_m > \bar{g}$. Indeed, on the real axis, the phase $\eta_\xi(\omega)$ winds up by an infinite number of 2π between $\omega = O(\bar{g})$ and $\omega = \infty$, while near the Matsubara axis, $\eta_\xi(\omega_m) = 0$ in this frequency range. The discrepancy implies that phase winding must end somewhere between the real and the Matsubara axis. We now argue that there is a set of vortices in the upper frequency half-plane, at $|z| \geqslant \bar{g}$ and the phase winding drops by 2π each time the axes of z passes through a vortex upon rotation away from the real axis.

We use the Cauchy relation

$$\Delta(z) = \frac{2}{\pi}\int_0^\infty dx\frac{x\Delta''(x)}{x^2 - z^2} \tag{58}$$

to extend the gap function $\Delta(x) = xD(x)$ from the real axis to complex $z = \omega' + i\omega''$ with $\omega'' > 0$. We use Eq. (56) for the gap function as we expect vortices to

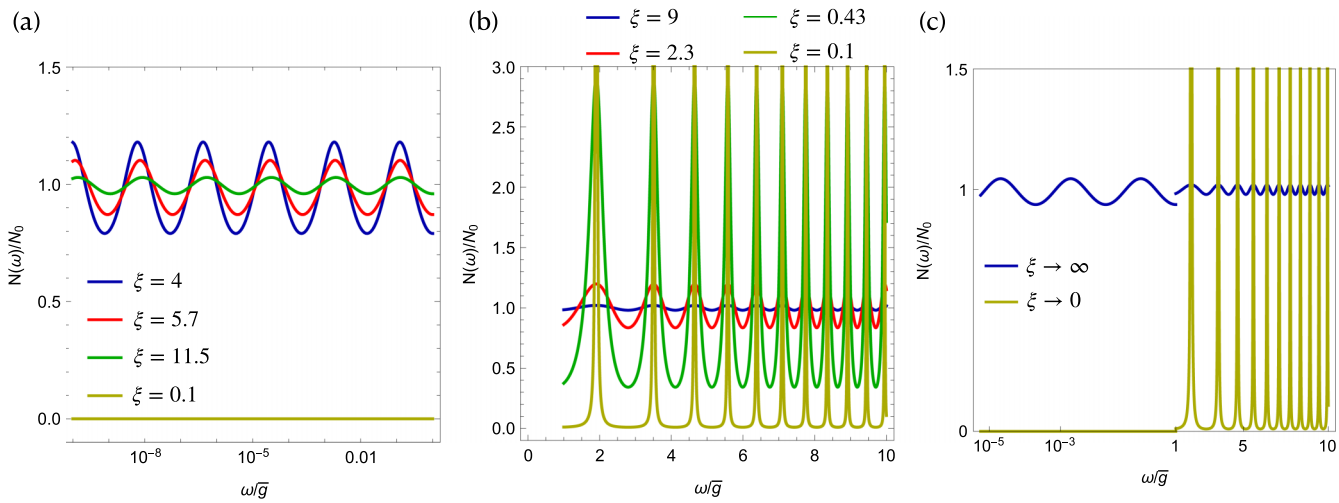

FIG. 8. DoS $N_\xi(\omega)$ for (a) $\omega < \bar{g}$ and (b) $\omega > \bar{g}$ and for different ξ. For all $\xi > 0$, $N_\xi(\omega)$ remains finite down to $\omega = 0$ (a gapless superconductivity). For $\xi = 0$, the DoS $N_0(\omega)$ vanishes at small ω and has a set of δ-functional peaks at $\omega > \bar{g}$. In (c), we present the schematic plot of the DoS at all frequencies.

be present at $|z| > \bar{g}$. Like before, we first consider the cases $\xi = 0$ and $\xi \to \infty$, and then extend the analysis to arbitrary ξ.

A. Case $\xi = 0$

Using the expansion near $\phi(\omega_p) = p\pi$, Eq. (51), we approximate $\Delta_0''(\omega)$ as

$$\Delta_0''(\omega) \approx \frac{\pi^2\bar{g}^2}{2} \sum_{p=1}^{\infty} \frac{(-1)^{p+1}\omega_p^2}{\omega_p^2 + \bar{g}^2} \delta(\omega - \omega_p). \tag{59}$$

Substituting into (58), we obtain

$$\Delta_0(z) = \pi\bar{g}^2 \sum_{p=1}^{\infty} \frac{(-1)^{p+1}\omega_p^3}{\omega_p^2 + \bar{g}^2} \frac{1}{\omega_p^2 - z^2}. \tag{60}$$

Here ω_p is a solution of $\phi_0(\omega_p) = \pi p$, where $\phi_0(\omega)$ is given by (49). We verified numerically that KK relations on the real axis are satisfied, i.e., if we use (59), we reproduce with high accuracy $\Delta'(\omega)$. On the Matsubara axis, $z = i\omega_m$, Eq. (60) yields, at $\omega_m \gg \bar{g}$,

$$\Delta_0(\omega_m) = a\frac{\bar{g}^3}{\omega_m^2}, \tag{61}$$

where $a = \pi \sum_{p=1}^{\infty} [(-1)^{p+1}\omega_p^3/((\omega_p^2 + \bar{g}^2)\bar{g})]$. Approximating ω_p by $\bar{g}\pi\sqrt{p}$, we find $a = 2.56$. The number is somewhat larger than 1.27, obtained by solving the gap equation on the Matsubara axis (Ref. [9] and Sec. III B). The difference likely comes from subleading terms in $\phi(\omega)$.

We plot $\Delta_0(z)$ for a generic z in the upper half-plane in Fig. 9 We clearly see that there is a set of points, where $\Delta_0'(z) = \Delta_0''(z) = 0$. These points are the centra of dynamical vortices with anticlockwise circulation 2π. The vortices are located along a particular line in the complex plane. The set extends to an infinite frequency, i.e., the number of vortices is infinite. This is consistent with an infinite phase winding along the real axis. We verified that if we use a more accurate form of ω_p, the positions of the vortices shift a bit, but their number remains infinite.

To see how the winding number changes once we rotate from the real to the Matsubara axis, we introduce $z = |z|e^{i\psi}$ ($\psi = 0$ along the positive real semi-axis and $\pi/2$ along the Matsubara axis) and check the winding of the phase of $\Delta_0(z) = |\Delta_0(z)|e^{i\eta_0(z)}$ between $|z| \sim \bar{g}$ and $|z| \to \infty$ along the directions in the upper frequency half-plane, specified by ψ. We show the results in Fig. 10.

We see that for any $\psi > 0$, the phase $\eta_0(z)$ winds for $|z|$ below a certain value, and then saturates. At larger $|z|$, both $\Delta_0'(z)$ and $\Delta_0''(z)$ scale as $1/|z|^2$ with no oscillations. Counting the total phase winding $\delta\eta_0$ between $|z| = O(\bar{g})$ and $|z| = \infty$, we see that $\delta\eta_0 = 2\pi s$, where s is an integer. It decreases by one every time the direction set by ψ passes through a vortex. The winding vanishes at some $\psi \leqslant \pi/4$.

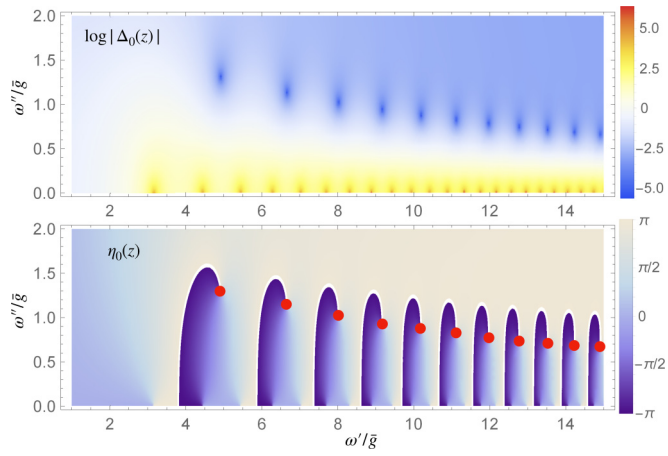

FIG. 9. $\Delta_0(z)$ in the upper half-plane. (Top) $\ln|\Delta_0(z)|$. Blue spots mark the locations of dynamical vortices, where $|\Delta_0(z)|$=0. (Bottom) The phase of the gap $\eta_0(z)$ defined via $\Delta_0(z) = |\Delta_0(z)|e^{i\eta_0(z)}$. The phase slips by 2π upon crossing a white line in the direction from near-white to dark-blue. The white lines are the locations of points where $\Delta_0''(z) = 0$ and $\Delta_0'(z) < 0$.

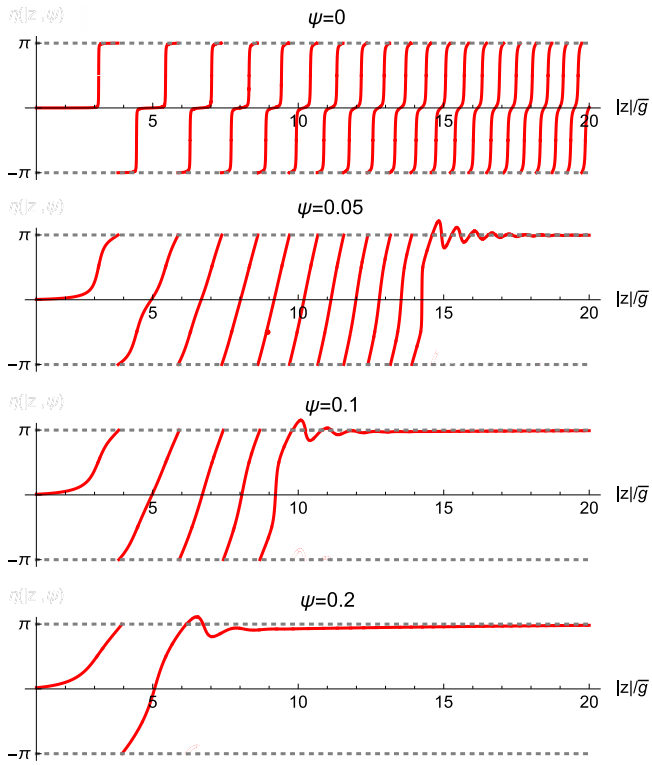

FIG. 10. Phase variation $\eta_0(|z|, \psi)$ along different paths specified by ψ, defined via $z = |z|e^{i\psi}$. Along real axis, $\psi = 0$; along Matsubara axis, $\psi = \pi/2$. Along the real axis the phase $\eta_0(\omega)$ winds up an infinite number of times, i.e., the winding number (the number of 2π phase slips) is infinite. For a finite ψ, phase winding ends at some finite $|z|$, and the winding number becomes finite.

B. Case $\xi = \infty$

We next consider the opposite limit $\xi = \infty$. The form of $\Delta_\infty(z)$ can be obtained starting from (15) and replacing ω_m^2 by $|z|^2 e^{i(2\psi-\pi)}$. This gives

$$\Delta_\infty(z) \propto \int_0^\infty dk (b_k e^{-ik \ln |z|^2/\bar{g}^2 + (2\psi-\pi)k} + b_{-k} e^{ik \ln |z|^2/\bar{g}^2 - (2\psi-\pi)k}), \quad (62)$$

where b_k is defined in (16). We obtain $\Delta_\infty(z)$ by numerical integration. We plot its phase $\eta_\infty(z)$ in Fig. 11. We again see that there is an infinite array of vortices. The array extends to an infinite frequency, where it approaches the real axis. The vortex arrangement in Fig. 11 is remarkable similar to that in Fig. 9 for $\xi = 0$. Moreover, if we approximate $\phi(\omega)$ by the leading term $(\omega/\bar{g})^2/\pi$, we find that the positions of the vortices are at the same z_i in both cases. We can see this by comparing Fig. 12(a) where $\xi \to \infty$ and Fig. 12(c) where $\xi \to 0$. The gap function $\Delta_\xi(z)$ are very similar in these two cases, despite that the overall factors are different. The vortex positions for these two cases are almost identical, as can be seen from Fig. 12(d).

C. Arbitrary ξ

The same infinite array of vortices exists for all $0 < \xi < \infty$. As an example, in Fig. 12(b) we show the gap function for

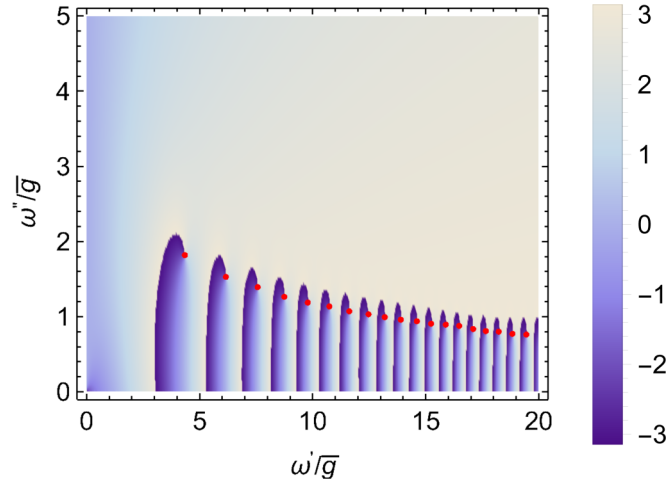

FIG. 11. The phase $\eta_\infty(z)$ of $\Delta_\infty(z)$ in the first quarter of the complex plane of frequency ($\omega' > 0$, $\omega'' > 0$).

$\xi = 1$. We clearly see that there is an infinite array of vortices, similar to the ones for $\xi = \infty$ and $\xi = 0$, and the positions of vortices are almost indistinguishable, see Fig. 12(d). Analytically, if we use Eqs. (56) and (58), we find that the positions of vortices are independent on ξ.

D. Essential singularity

There is another consequence of the existence of an infinite array of vortices – each gap function $\Delta_\xi(z)$ has an essential singularity at $|z| = \infty$. Indeed, one can reach $|z| = \infty$ from the set of vortex points, where $\Delta_\xi(z) = 0$, or from the real axis, where $\Delta_\xi(\omega)$ oscillates, and the amplitude of the oscillations does not vanish at $\omega \to \infty$, hence neither $\lim_{|z|\to\infty} \Delta_\xi(|z|)$ nor $\lim_{|z|\to\infty} 1/\Delta_\xi(|z|)$ exist. We emphasize that an essential singularity is only present for $\gamma = 2$. For smaller γ, phase winding and associated vortices exist only at $|z|$ smaller than a certain, $\gamma-$ dependent value. At larger $|z|$, $\Delta(z)$ scales as $1/|z|^\gamma$ and vanishes at $|z| = \infty$ no matter how this limit is reached.

Further, for $\gamma = 2$, the very existence of a nonzero $\Delta_\xi(z)$ for a generic z away from vortex points, is ultimately related to an essential singularity at $|z| = \infty$. The argument is that the set of vortex points is complete, hence one can analytically continue the gap function from this set to the upper half-plane of frequency in the same way as $\Delta(z)$ is obtained from a discrete set of Matsubara points $\omega_m = \pi T(2m + 1)$ in standard diagrammatic calculations for interacting fermions. If this analytical continuation was unique, we would obtain $\Delta(z) \equiv 0$, because $\Delta(z) = 0$ at the vortex points. For a nonzero $\Delta_\xi(z)$, the extension must be multi-valued. A rigorous mathematical argument is that this is the case when the end point of the set, $|z| = \infty$, goes outside the domain of analyticity. This is exactly what we have because of an essential singularity at $|z| = \infty$.

We conjecture that the multi-value nature of the extension is the reason why the set of $\Delta(\omega)$ is a continuous one at $\gamma = 2$. This is plausible, particularly if the vortices are at the same z_i for all ξ, as Fig. 12 seems to indicate. However, at the moment, we cannot prove this.

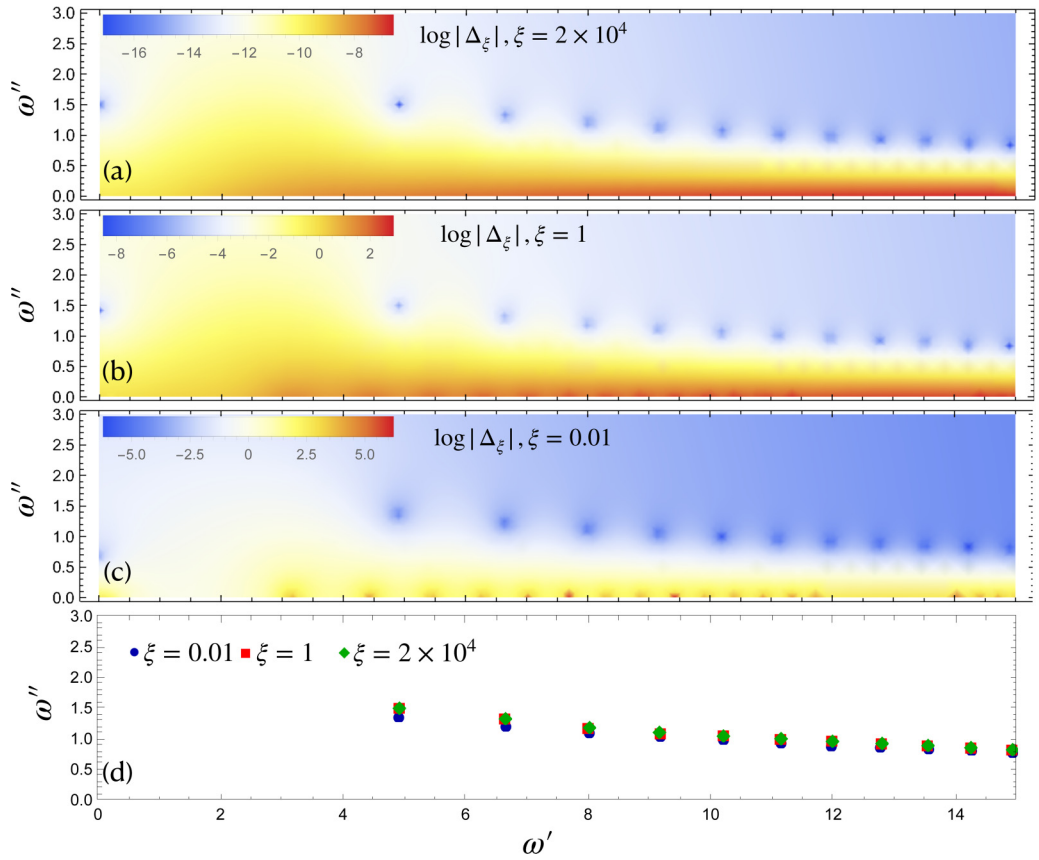

FIG. 12. [(a)–(c)] Gap functions Δ_ξ defined in (56) for different ξ in the frequency upper half-plane. Here we take $\phi(\omega) \approx (\omega/\bar{g})^2/\pi$. (d) Comparison of the vortex positions for different ξ obtained by approximating $\phi(\omega)$ by $(\omega/\bar{g})^2/\pi$. The results suggest that the positions of the vortices almost do not depend on the value of ξ.

VI. FINITE ω_D

A. Gap equation at a finite ω_D

We now consider the case when the bosonic mass is small but finite. By analogy with the phonon case we call this mass ω_D. On the Matsubara axis, $\Delta_0(\omega_m)$ changes little compared to the case $\omega_D = 0$. The set of $\Delta_n(\omega_m)$ still exists at small ω_D, but becomes discrete and holds up to a finite $n_{\max}$. In particular, there is no solution of the linearized gap equation at $T = 0$ for any nonzero ω_D. The value of $n_{\max}$ can be estimated by noticing that if we, e.g., depart from the solution on the Matsubara axis at $\omega_D = 0$ and compute corrections due to finite ω_D, these corrections increase at small ω_m and become $O(1)$ at $\omega_m \sim \omega_D$. A simple experimentation shows that this sets $n_{\max}$ at

$$n_{\max} \sim \frac{\bar{g}}{\omega_D}. \tag{63}$$

On the real axis, the gap equation still has the form $D(\omega)\omega B(\omega) = A(\omega) + C(\omega)$, and $A(\omega)$ and $B(\omega)$ remain the same as in (8), up to irrelevant small corrections. However, $C(\omega)$ changes to

$$C(\omega) = -i\frac{\pi\bar{g}^2}{2\omega_D}\frac{D(\omega-\omega_D) - D(\omega)}{\sqrt{1 - D^2(\omega-\omega_D)}}\mathrm{sgn}\omega. \tag{64}$$

Expanding to first order in ω_D and introducing, as before, $D(\omega) = 1/\sin\phi(\omega)$, we obtain after straightforward algebra that the gap equation reduces to

$$\dot{\phi} - \frac{\omega_D}{2}((\dot{\phi})^2\tan\phi(\omega) + \ddot{\phi}) = \frac{2}{\pi\bar{g}^2}[\omega B(\omega) - A(\omega)\sin\phi(\omega)] + \cdots, \tag{65}$$

where dots stand for the terms with higher powers of ω_D. A similar equation at a finite T instead of finite ω_D has been obtained by Combescot [9].

For definiteness, let's consider the case $\xi = 0$. At $\omega \geqslant \bar{g}$, $B(\omega)$ and $A(\omega)$ from (8) can be approximated by $B(\omega) \approx 1 + \bar{g}^2/\omega^2$ and $A(\omega) \approx -1.27\bar{g}^3/\omega^2$. To understand the effect of ω_D we use as an input the solution at $\omega_D = 0$, $\phi(\omega) \approx \omega^2/(\pi\bar{g}^2) + i\delta$. Substituting this input into (65), expanding near $\omega = \pi\bar{g}/\sqrt{2}$, where $\phi(\omega) = \pi/2$, expressing $\phi(\omega) = \phi'(\omega) + i\phi''(\omega)$, and solving for $\phi''(\omega)$, we find that it jumps to $O(\omega_D)$ once ω exceeds $\pi\bar{g}/\sqrt{2}$. The same happens at all $\omega_n = \pi\bar{g}/\sqrt{2}(2n+1)^{1/2}$, where $\tan\phi'(\omega) = 0$. After n jumps, $\phi''(\omega)$ becomes

$$\phi''(\omega) = \frac{\pi\omega_D}{\sqrt{2}\bar{g}}\sum_{m=1}^{n}\sqrt{2m+1} \approx \frac{2\pi\omega_D}{3\bar{g}}n^{3/2} \approx \frac{2\omega_D}{3\pi^2}\frac{\omega^3}{\bar{g}^4}. \tag{66}$$

A more accurate, nonperturbative analysis of (65) shows that $\phi''(\omega)$ appears slightly before $\phi'(\omega)$ reaches $\pi/2$. This smoothes up the jumps, but the functional form of $\phi''(\omega)$ in (66) remains intact. When both ϕ' and ϕ'' are non-zero, $D(\omega)$

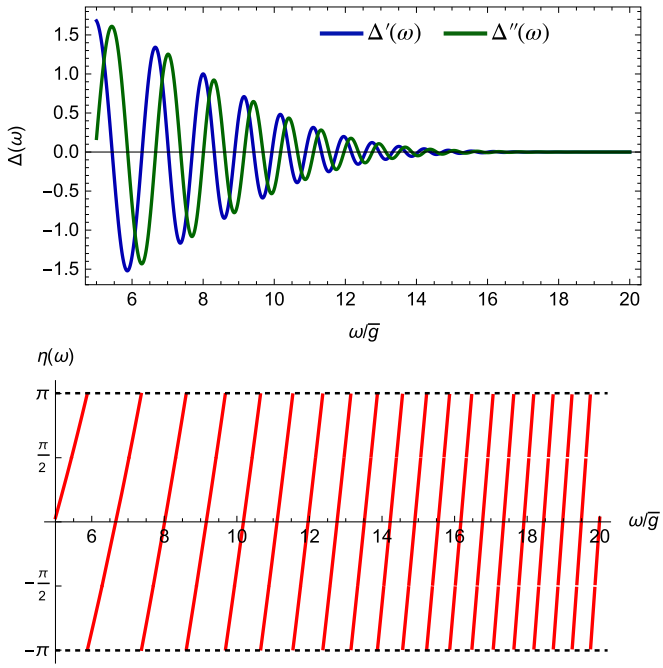

FIG. 13. The gap function $\Delta(\omega)$ (a) and the variation of its phase $\eta(\omega)$ at $\omega_D = 0.02\bar{g}$. From (69).

is a complex function of frequency:

$$D_0'(\omega) = \omega \frac{\sin\phi'(\omega)\cosh\phi''(\omega)}{\sin^2\phi'(\omega) + \sinh^2\phi''(\omega)} \mathrm{sgn}\omega \tag{67}$$

and

$$D_0''(\omega) = -\omega \frac{\cos\phi'(\omega)\sinh\phi''(\omega)}{\sin^2\phi'(\omega) + \sinh^2\phi''(\omega)} \tag{68}$$

At $\omega > 3\pi^2\bar{g}^4/(2\omega_D)$, $\phi''(\omega)$ becomes larger than one. At such frequencies, both $D'(\omega)$ and $D''(\omega)$ oscillate with progressively decreasing magnitudes, approximately as the real and the imaginary parts of

$$-2ie^{i\omega^2/(\pi\bar{g}^2)} e^{-\frac{2\omega_D}{3\pi^2\bar{g}}(\omega/\bar{g})^3}, \tag{69}$$

and the phase $\eta_0(\omega)$ gradually winds up as ω increases. We show this in Fig. 13. This behavior holds as long as $|A(\omega)| \ll \omega$, i.e., $\omega < \omega_{\max}$, where

$$\omega_{\max} \sim \bar{g}\left(\frac{\bar{g}}{\omega_D}\ln\frac{\bar{g}}{\omega_D}\right)^{1/3}. \tag{70}$$

At even larger frequencies, the $A(\omega)$ term cannot be neglected, and the forms of $\phi'(\omega)$ and $\phi''(\omega)$ change. We show the full numerical solution of Eq. (65) in Fig. 14. We see that at $\omega > \omega_{\max}$, $\phi''(\omega)$ keeps increasing, while $\phi'(\omega)$ saturates. A simple analysis shows that Eq. (65) is satisfied, up to corrections of order ω_D, if

$$\phi''(\omega) = 3\ln\frac{\omega}{\bar{g}} + 0.45, \quad \phi'(\omega) = -\frac{\pi}{2} + 2m\pi, \tag{71}$$

where m is an integer. Substituting this complex $\phi(\omega)$ into $\Delta_0(\omega) = \omega/\sin\phi(\omega) \approx -2i\omega e^{i\phi(\omega)}$, we see that at $\omega > \omega_{\max}$, the real part of the gap function gradually decreases as

$$\Delta_0'(\omega) = \frac{1.27\bar{g}^3}{\omega^2}. \tag{72}$$

To obtain $\Delta_0''(\omega)$ at these frequencies, we need to keep the ω_D term in the l.h.s. of (65) and obtain the correction to (71), which we label as $\tilde{\phi}$. Solving perturbatively for $\tilde{\phi}(\omega)$, we obtain

$$\tilde{\phi}(\omega) = f\left(\frac{\omega}{\omega_{\max}}\right) e^{i\omega^2/(\pi\bar{g}^2)}, \tag{73}$$

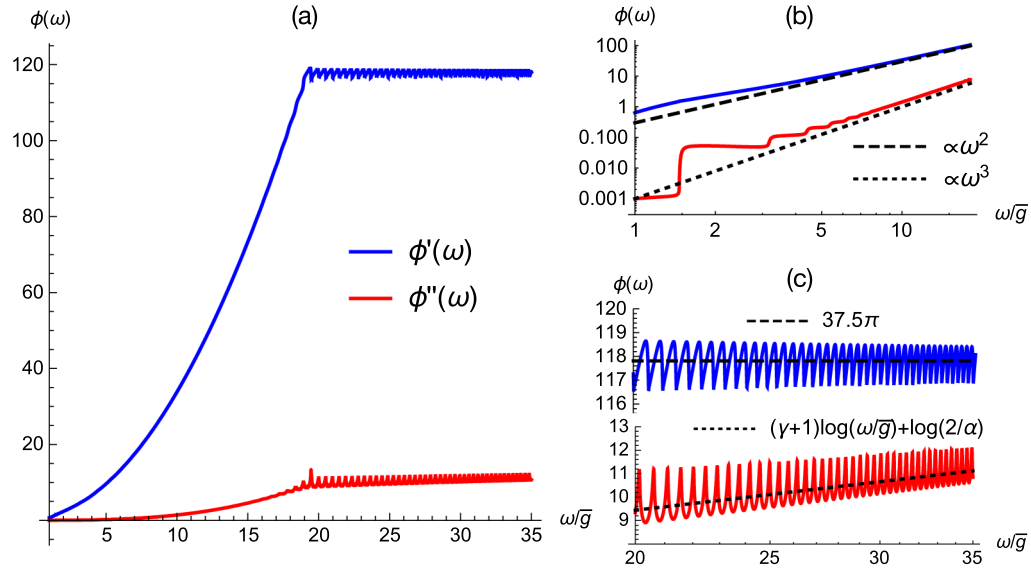

FIG. 14. (a) Numerical solution of Eq. (65) for a complex $\phi(\omega)$ at $\omega_D = 0.02\bar{g}$. [(b) and (c)] Asymptotic forms of $\phi'(\omega)$ and $\phi''(\omega)$. At $\omega < \omega_{\max}$, $\phi'(\omega)$ increases as ω^2, while $\phi''(\omega)$ first displays a step-like behavior and then increases as ω^3, with ω_D in the prefactor. At $\omega > \omega_{\max}$, $\phi'(\omega)$ saturates at $(2m-1/2)\pi$, where $m = 19$ for our chosen ω_D, and $\phi''(\omega)$ increases logarithmically. The corrections to asymptotic values oscillate with the period set by ω^2/π. In the numerical solution, we neglected $\ddot{\phi}$ term in (65) compared to $(\dot{\phi})^2$ and verified that this is a valid approximation.

where $f(\dots)$ is a decreasing function of the argument. The ω^2 oscillations of $\tilde{\phi}(\omega)$ are clearly visible in the numerical results for ϕ' and ϕ'' in Fig. 14. Substituting (73) into (68), we obtain

$$\Delta_0''(\omega) \sim \frac{\bar{g}^3}{\omega^2} f\left(\frac{\omega}{\omega_{\max}}\right) \cos\frac{\omega^2}{\pi\bar{g}^2}. \tag{74}$$

One can verify that an integer m in (71) determines the number of 2π variations of $\eta_0(\omega)$ on the real axis and, equivalently, the number of vortices at complex z_i. The value of m decreases one-by-one as ω_D increases and $\omega_{\max}$ decreases. That m is finite implies that there is no essential singularity at $|z| = \infty$. Indeed, at the largest frequencies, $\Delta(\omega) \propto 1/\omega^2$.

For completeness, we verified that higher-order terms in ω_D, which we neglected in the l.h.s. of (65), become important at frequencies $\omega \sim \bar{g}^2/\omega_D$, which well exceed $\omega_{\max}$ and are therefore irrelevant to our purposes.

VII. DRESSED SUPERFLUID STIFFNESS

In this section, we analyze superfluid stiffness and thermal corrections to a superconducting order parameter. As we discussed in Introduction, we consider the $\gamma = 2$-model as the double limit $\omega_D \to 0$, $E_F \to \infty$, such that Migdal-Eliashberg parameter $\lambda_E = \bar{g}^2 N_0/\omega_D$ remains small ($N_0 \sim 1/E_F$ is the DoS per unit volume in the normal state). Accordingly, in the analysis below we keep ω_D small, but finite.

A. Bare stiffness

A superfluid stiffness is the ratio of the excess energy E_η due to inhomogeneous variation of the phase of a superconducting order parameter $\Delta(r) = \Delta e^{i\eta(r)}$ and $\int dr(\nabla\eta(r))^2$: $E_\eta = \rho_s \int dr(\nabla\eta(r))^2$. In the momentum space,

$$E_\eta = \rho_s \sum_q q^2 \eta_q^2. \tag{75}$$

A way to compute ρ_s is to choose $\eta_q = \delta_{q,q_0}$ and extract ρ_s as the prefactor for q_0^2 term in the particle-particle bubble (the sum of GG and FF terms) at zero frequency and finite q (see Refs. [28,30,38]).

At $\omega_D/\bar{g} > 1$, the system is in a weak coupling limit, and superfluid stiffness at $T = 0$ is a fraction of the Fermi energy, $\rho_s(T = 0) = E_F/(4\pi)$ (Refs. [28,30]). This stiffness is much larger than T_c [39]. At $T > 0$, $\rho_s(T)$ drops and vanishes at T_c, but at weak coupling a drop of ρ_s occurs only in the immediate vicinity of T_c.

At small $\omega_D/\bar{g}$, strong mass renormalization $m^*/m = 1 + \bar{g}^2/\omega_D^2$ changes the stiffness to

$$\rho_s(T = 0) \sim E_F \frac{\omega_D \Delta(0)}{\bar{g}^2} \sim \frac{T_p}{\lambda_E}, \tag{76}$$

where $T_p \sim \Delta(0)$ is the onset temperature of the pairing. As long as $\lambda_E \leqslant 1$, $\rho_s(T = 0) > T_p$.

We now relate the stiffness to the strength of thermal phase fluctuations of $\Delta(r) = \Delta e^{i\eta(r)}$. For this, consider the correlator

$$\langle\eta(r)\eta(0)\rangle = \frac{\int D[\eta]\eta(r)\eta(0)e^{-\rho_s\int dr(\nabla\eta(r))^2/T}}{\int D[\eta]e^{-\rho_s\int dr(\nabla\eta(r))^2/T}}. \tag{77}$$

We assume that in equilibrium $\eta(r) = 0$ and expand $\langle e^{i\eta(r)}\rangle$ as $1 - \langle\eta^2(r)\rangle/2$. Transforming (77) to the momentum space, we obtain $\langle\Delta(r)\rangle = \Delta(1 - \langle\eta^2\rangle)$, where

$$\langle\eta^2\rangle = \frac{1}{N}\sum_q \frac{\prod_{q'}\int d\eta_{q'}\eta_q^2\, e^{-\rho_s q^2\eta_{q'}^2/T}}{\prod_{q'}\int d\eta_{q'}\, e^{-\rho_s q^2\eta_{q'}^2/T}}, \tag{78}$$

where N is the number of particles in the system. Evaluating the integrals, we obtain the conventional result [40]

$$\langle\eta^2\rangle = \frac{T}{\rho_s}\frac{1}{N}\sum_q \frac{1}{q^2}. \tag{79}$$

We assume for simplicity that spatial dimension D is larger than 2, in which case the sum converges. By order of magnitude we then have

$$\langle\eta^2\rangle \sim \frac{T}{\rho_s(T)}. \tag{80}$$

As long as $\rho_s(T) > T$, fluctuation corrections to the order parameter are small. This does not hold in the immediate vicinity of the onset temperature of the pairing, T_p, but as long as $\rho_s(0) \gg T_c$, the T range, where fluctuations are strong and destroy phase coherence, is quite narrow, i.e., superconducting T_c remains close to T_p. We see that this holds even when ω_D is small and the reduction of ρ_s by mass renormalization is strong.

B. Dressing of ρ_s by soft longitudinal fluctuations

We now argue that in our case the expression for $\langle\eta^2\rangle$ is different due to the presence of a continuum gapless spectrum of condensation energy, $E_{c,\xi}$, where, we remind, ξ runs between 0 and ∞, and the bottom of the spectrum is at $\xi = 0$. We will need states near the bottom of the continuum, at $\xi \ll 1$. For such states, we assume

$$E_{c,\xi} = E_{c,0} + b_1 N_0 N \bar{g}^2 \xi^2, \tag{81}$$

where $b_1 = O(1)$ and N is the total number of particles. We will also need superfluid stiffness $\rho_{s,\xi}$ for the states near the bottom of the continuum. Evaluating the particle-particle susceptibility for a generic $\Delta_\xi(\omega_m)$ and extracting the q^2 term, we obtain

$$\rho_{s,\xi} \sim E_F \frac{\omega_D}{\bar{g}^2}\int d\omega_m \frac{D_\xi^2(\omega_m)}{1 + D_\xi^2(\omega_m)}. \tag{82}$$

For $\xi = 0$, the integral is determined by $\omega_m \sim \bar{g}$, where $D_0(\omega_m) \sim 1$. This yields $\rho_{s,0} \sim E_F\omega_D/\bar{g} \sim T_p/\lambda_E$, as in (76). For states with $\xi > 0$, the magnitude of $\Delta_\xi(\omega_m)$ is reduced, and the stiffness gets smaller. We assume that for the states near the bottom of the continuum, the stiffness is obtained by expanding to first order in ξ:

$$\rho_{s,\xi} = \rho_{s,0}(1 - b_2\xi), \tag{83}$$

where $b_2 = O(1)$ is positive. The extra energy of a given state ξ due to phase variation is

$$E_{\eta,\xi} = \rho_{s,\xi}\sum_q q^2\eta_q^2. \tag{84}$$

We assume (see reasoning below) that all states near the bottom of a continuum contribute to the variation of the phase,

i.e., the averaging in $\langle(\eta_q)^2\rangle$ is over both η_q and ξ with the weight factor $e^{-E_\xi/T}$, where

$$E_\xi = E_{c,\xi} + E_{\eta,\xi} = E_0 + \delta E_\xi \tag{85}$$

and

$$E_0 = E_{c,0} + \rho_{s,0}\sum_q q^2\eta_q^2,$$

$$\delta E_\epsilon = b_1 N_0 g^2\xi^2 - b_2\rho_{s,0}\xi\sum_q q^2\eta_q^2. \tag{86}$$

If we neglected δE_ξ, we would obtain the same result as before:

$$\langle\eta^2\rangle = \frac{T}{\rho_{s,0}}\frac{1}{N}\sum_q\frac{1}{q^2}. \tag{87}$$

Keeping δE_ξ we find that $\langle\eta^2\rangle$ has an additional overall factor, which we label as I_T. Dropping for simplicity numerical prefactors b_1 and b_2, we obtain after integrating over $\eta_{q'}$

$$I_T = \frac{\int d\xi e^{-Nf(\xi)\frac{1}{1-\xi}}}{\int d\xi e^{-Nf(\xi)}}, \tag{88}$$

where

$$f(\xi) = \frac{N_0\bar{g}^2}{T}\xi^2 - \frac{\xi}{2}. \tag{89}$$

We assume that the measure of the integration over ξ is nonsingular. The linear in ξ term in $f(\xi)$ comes from integration over $\eta_{q'}$ with $q' \neq q$ [see Eq. (78)]. Each integration over q' yields $1/\sqrt{1-\xi}$, and the product of the integrals over all q' yields $1/(1-\xi)^{N/2} = e^{-(N/2)\ln(1-\xi)} \approx e^{(N/2)\xi}$.

At small T, the function $f(\xi)$ in (89) has a minimum at $\xi{=}T/(4N_0\bar{g}^2) \sim T/(4\omega_D\lambda_E)$. Then $I_T{=}1/(1-T/(4\omega_D\lambda_E))$ and

$$\langle\eta^2\rangle \sim \frac{T\lambda_E}{T_p}\frac{1}{1-\frac{T}{4\omega_D\lambda_E}}. \tag{90}$$

We see that the renormalizations coming from the low-energy states of the continuum spectrum of the condensation energy hold in powers of T/ω_D. With these renormalizations, the fully dressed stiffness is

$$\rho_s(T) = \frac{T_p}{\lambda_E}\left(1 - \frac{T}{4\omega_D\lambda_E}\right). \tag{91}$$

We see from that the value of $\rho_s(T)$ at $T \to 0$ and $\omega_D \to 0$ depends on the order of limits. At $T = 0$, $\rho_s(0) = T_p/\lambda_E$ is finite and exceeds T_p. At $\omega_D \to 0$, the corrections to stiffness rapidly increase with T, and $\rho_s(T)$ becomes comparable to T at $T \sim \omega_D\lambda_E$. For the largest $\lambda_E \sim 1$, at which our theory is valid, this holds at $T \sim \omega_D$. It is tempting to associate this temperature with the actual T_c above which the system looses long-range phase coherence.

Further, there is an analogy between finite ω_D and finite $2-\gamma$, as the two have similar effect on the gap function (see paper IV). Replacing ω_D by $\bar{g}(2-\gamma)$, we find that at $\omega_D = 0$ and $\gamma < 2$, superconducting $T_c \sim \bar{g}(2-\gamma)$.

Before concluding this Section, we elaborate on our assumption that the averaging over phase fluctuations should include low-energy states from the continuum spectra of the condensation energy. Consider the case $\gamma < 2$, when the spectrum is still discrete and the $n = 0$ solution has the lowest condensation energy $E_{c,0}$. The energies $E_{c,n\geqslant 1}$ are close to $E_{c,0}$, yet the solutions with different n are topologically distinct as $\Delta_n(\omega_m)$ has n vortices. These other states contribute to the renormalization of the phase of $\Delta_0(\omega_m)$ only if the tunneling amplitude between the states $n = 0$ and $n > 0$ is nonzero, which requires the barrier between $E_{c,0}$ and $E_{c,n}$ to be small. The height of the barrier depends on the path along which a state without a vortex transforms into a state with a vortex at some small ω_m. A vortex can either come from $\omega_m = \infty$, in which case the barrier is high, or via a creation of a vortex-antivortex pair at $\omega_m = 0$, in which case it is low. For a generic $\gamma < 2$, $\Delta_n(z)$ are regular at small z in the complex plane, hence one should not expect an antivortex nearby. However, for $\gamma \to 2$, our candidate $\Delta_\xi(z)$, Eq. (38), possess antivortices at small z in the lower frequency halfplane. In this situation, it is natural to expect that, the barriers between $E_{c,0}$ and $E_{c,n}$ with $n > 0$ are low, hence our reasoning is justified.

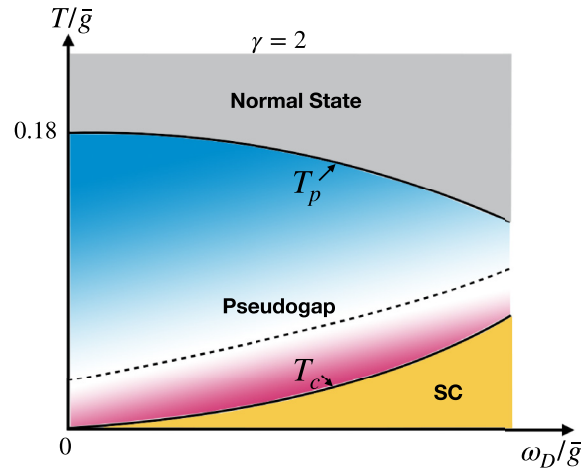

FIG. 15. The phase diagram of the γ model for $\gamma = 2$ in variables $(T/\bar{g}, \omega_D/\bar{g})$, where ω_D is the mass of a pairing boson. T_p is the onset temperature of the pairing, and T_c is the actual superconducting transition temperature, below which the system establishes phase coherence. In between the system displays pseudogap behavior, in which fermionic pairs are formed, but there is no macroscopic phase coherence. The dashed line separates the two regimes within the pseudogap phase – the one at higher T, where the system behavior is chiefly determined by fermions with the two lowest Matsubara frequencies $\pm\pi T$, and the one at lower T, when fermions with all Matsubara frequencies contribute to the pairing. In these two regimes the system displays gap filling and gap closing behavior, respectively.

VIII. PHASE DIAGRAM OF THE γ MODEL

A. $\gamma = 2$, finite ω_D

In Fig. 15, we present the phase diagram for $\gamma = 2$ for nonzero ω_D and T. At $\omega_D = 0$, the true transition temperature into a SC state is zero, although the onset temperature for the pairing, T_p is finite. At finite ω_D, T_c is finite but much smaller than T_p, at least for small ω_D. In between T_c and T_p, the system displays pseudogap behavior: The spectral

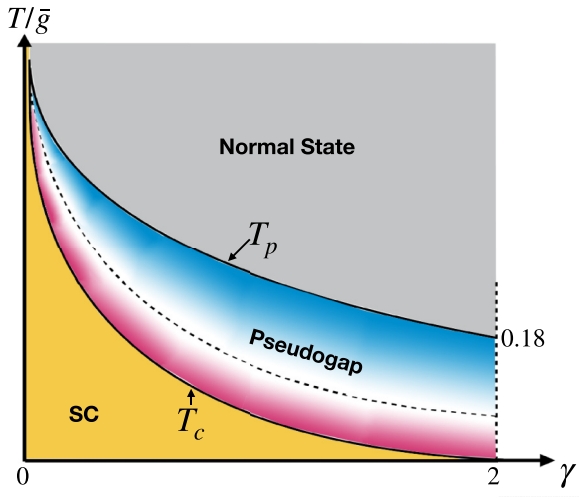

FIG. 16. The phase diagram of the γ model for a generic $\gamma < 2$ at a finite T and vanishing ω_D. For any $\gamma < 2$, the true SC transition temperature T_c is finite, but is smaller than the onset temperature for the paring, T_p. In between T_c and T_p, the system displays a pseudogap behavior. There are two distinct behaviors in the pseudogap regime, like in Fig. 15: close to T_p, the spectral function and the DoS display gap filling behavior, while close to T_c, the behavior becomes more conventional and the gap frequency shifts to a smaller value as T increases.

function and the DoS display a peak at a finite frequency, but the spectral weight below the peak remains finite. Close to T_p, the pairing is mainly induced by fermions with the two lowest Matsubara frequencies $\pm\pi T$ (Refs. [43,44,49]). In this situation, the position of the peak in the spectral function and the DoS increases linearly with T, and the gap fills in as T approaches T_p. In the T range near T_c, fermions with all Matsubara frequencies contribute to the pairing, and the positions of the maxima in the spectral function and the DoS move to smaller frequencies as T increases (gap closing behavior). We show the DoS in the two regimes in Fig. 18 below.

B. $\omega_D = 0, 0 < \gamma \leqslant 2$

In Fig. 16, we show the phase diagram for the γ model with $0 < \gamma \leqslant 2$, at $\omega_D = 0$ and finite T. This phase diagram is based on the results of this work and previous works (papers I–IV). For $\gamma < 2$, we found earlier the largest condensation energy is for sign-preserving solution of the gap equation ($n = 0$ in our classification). Still, for any $\gamma > 0$, there exists an infinite set of topologically distinct solutions for the gap (all with the same symmetry), labeled by integer n. This generates a discrete spectrum of the condensation energy $E_{c,n}$. The spectrum is sparse near the bottom at small γ, but becomes dense and flattens up at the bottom as γ approaches 2. At $\gamma \leqslant 2$, the corrections to superconducting order parameter from the states with $n \neq 0$ are small at low T, but rapidly increase with increasing T and destroy phase coherence at $T_c \sim \bar{g}(2-\gamma)/\lambda_E$. For $\gamma \leqslant 2$, $T_c \ll T_p$, and there exists a wide intermediate temperature range where the system displays a pseudogap behavior. By continuity, we expect that the pseudogap region to exist for all $\gamma > 0$ albeit with a smaller width.

C. Properties of the pseudogap phase

1. *toy model for $\gamma = 2$*

Let's start with $\gamma = 2$. At $T = 0$ the DoS is the set of δ functions [Fig. 17(a)]. At a finite T, two new features appear. First, $\Delta_0(\omega)$ decreases with increasing ω and displays no oscillations above $\omega_{\max}$, similar to the case with finite ω_D discussed in Sec. VI. As a result, δ-functional peaks in the DoS at larger frequencies get broadened and eventually disappear. Second, other $D_\xi(\omega)$ from the continuum spectrum of condensation energies contribute to the DoS with Boltzmann factors. For all these solutions, $\mathrm{Im}\Delta_\xi(\omega)$ remains finite down to $\omega = 0$. As a result, the DoS also becomes nonzero at the smallest ω (this phenomenon is often called a gapless superconductivity [31,32,41,42]) We model both effects by introducing a phenomenological $\Delta(\omega) = \omega/\sin(ia + (\omega/\bar{g})^2(1+ib))$, where a and b increase with T. We show the corresponding DoS in Figs. 17(b) and 17(c).

2. *Gap filling versus gap closing*

We argue, based on earlier works [43,44], that there are two different regimes of system behavior within the pseudogap phase. At low T, the position of the peak in the DoS scales with $\Delta_0(0)$ and decreases as T increases (the gap "closes" with increasing T). At higher T, the peak in the DOS shifts to higher frequencies and the spectral weight below the peak increases (gap "fills in" with increasing T). We illustrate this in Fig. 18. This last behavior is at least partly related to the fact that in some finite range of T below T_p, the gap function on the Matsubara axis is strongly peaked at the first Matsubara frequencies $\pm\pi T$ (Refs. [43,44]). On the real axis, the corresponding $\Delta(\omega)$ displays ω/T scaling. For such $\Delta(\omega)$, the peak frequency in the DoS increases linearly with T.

At a finite ω_D and/or $2-\gamma$, the "gap filling" behavior holds in some range between the onset temperature of the pairing T_p and a finite superconducting T_c (Fig. 18). To estimate the crossover temperature between the two regimes, we compare the actual T_p with the one obtained by neglecting the contributions from fermions with $\omega_m = \pm\pi T$. We show the results in Fig. 19. We see that for $\gamma = 2$ the onset temperature without $\pm\pi T$ fermions is strongly reduced – it is about 1/7 of the actual $T_p \sim 0.18\bar{g}$. This implies that the "gap filling" behavior holds in a wide range below T_p and crosses over to "gap closing" behavior only near T_c.

IX. CONCLUSIONS

In this paper, we extended our earlier analysis of the γ model to $\gamma = 2$. The $\gamma = 2$ model describes, among other cases, the pairing, mediated by an Einstein boson, in the limit when the bosonic mass ω_D tends to zero. On the real axis, the effective interaction in this limit $V(\Omega) = -\bar{g}^2/\Omega^2$ is repulsive, and, at a first glance, should not give rise to pairing. However, the same interaction on the Matsubara axis, $V(\Omega_m) = \bar{g}^2/\Omega_m^2$, is attractive, and earlier calculations on the Matsubara axis found that the onset temperature of the pairing, T_p, tends to a finite value $T_p = 0.1827\bar{g}$ at $\omega_D \to 0$ ($T_p = 0.1827\omega_D\sqrt{\lambda}$ in terminology of Ref. [14], which is the same expression because $\lambda = \bar{g}^2/\omega_D^2$). The issue we discussed

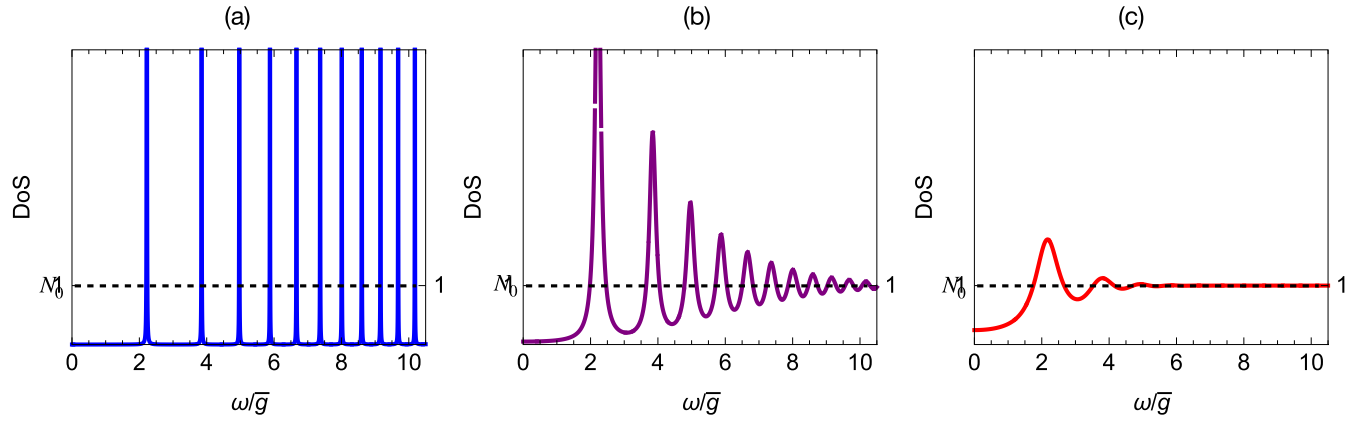

FIG. 17. The density of states, $N(\omega)$, at different temperatures, for a toy model with $\Delta_0(\omega) = \omega/\sin(ia + \omega^2(1 + ib))$, where a and b are two parameters, which increase with T. (a) The $T = 0$ limit, $a = b = 10^{-4}$. The DoS has a set of δ-functional peaks. (b) A finite but small T, $a = b = 0.05$. The first few peaks are well defined, but the peaks at large frequencies get overdamped and disappear. (c) A higher temperature, $a = b = 0.25$. The peak at the smallest frequency is still present, at about the same frequency as at $T = 0$, but other peaks are washed out, and the spectral weight below the peak increases, i.e., the DoS at low frequencies fulls in.

in this paper is whether this T_p is close to the actual superconducting T_c, or T_c is smaller, and there is a range of pseudogap behavior between T_c and T_p. We argued that the actual T_c scales with ω_D and is much smaller than T_p when $\omega_D/\bar{g}$ is small.

To prove this, we solved the nonlinear gap equation at $T = 0$ and $\omega_D = 0$ and found a continuum of solutions, governed by a single parameter ξ ($0 \leqslant \xi \leqslant \infty$). This in turn gives rise to a continuum spectrum of condensation energy, $E_{c,\xi}$, which can be viewed as a continuum gapless spectrum of "longitudinal" gap fluctuations. An infinite set of the gap functions and the condensation energies exists already for $\gamma < 2$, but is a discrete one. For $\gamma = 2$, this spectrum becomes continuous in a manner similar to how a discrete set of energy levels in a finite size crystal becomes a continuous vibration spectrum when system size becomes infinite. In our case, $1/(2 - \gamma)$ plays the role of a system size.

Without the contribution from the gapless longitudinal branch, superfluid stiffness $\rho_s(T = 0)$ is larger than T_p, and thermal corrections to superconducting order parameter scale approximately as $T/\rho_s(0)$ and remain small at all $T < T_p$. However, upon including contributions from the longitudinal branch, we found that thermal corrections become of order one already at much smaller $T \sim \omega_D$. We identified this temperature with the actual superconducting T_c. We emphasize that T_c vanishes at $\omega_D = 0$, and the behavior of the stiffness depends on the order in which the double limit $\omega_D \to 0$ and $T \to 0$ is taken. This strongly suggests that the $\gamma = 2$ model is critical at $T = 0$. At smaller γ, the ground state is not critical at $\omega_D = 0$, and $T_c \sim \bar{g}(2 - \gamma)$. It is finite but at $\gamma \leqslant 2$ is still much smaller than $T_p \sim \bar{g}$.

We presented collaborative evidence that the $\gamma = 2$ model is critical, from the analysis of the continuum set of gap functions along real frequency axis and in the upper half-plane of frequency. We found that for each solution, there is an infinite array of 2π vortices in the upper frequency half-plane. The array of vortices stretches up to an infinite frequency, where each gap function from the continuous set has an essential singularity. We speculated that different gap functions from the continuous set are different extensions from the array of vortices, onto the upper half-plane of frequency.

At a finite ω_D, the set of gap functions becomes discrete and contains only a finite number of solutions, all of which behave regularly in the high-frequency limit. The number of vortices also becomes finite. Still, at small $\omega_D/\bar{g}$, the system behavior over a wide frequency range mimics that at $\omega_D = 0$.

We showed the phase diagram of the $\gamma = 2$ model in variables T and ω_D in Fig. 15 and the phase diagram of the γ model at $\omega_D = 0$ in in variables T and γ in Fig. 16. In both cases, there is range of pseudogap behavior between the onset temperature of the pairing T_p and the actual T_c. In the pseudogap region, the bound pairs are formed, but there is no macroscopic phase coherence. We argued that in most of the pseudogap regime, the DoS and other observables display "gap filling" behavior, in which the peak position remains at a finite frequency up to T_p, while the states below the peak gradually fill in.

In the next (last) paper in the series, we consider the behavior of the γ model for $\gamma > 2$ and show that the new physics emerges at $T = 0$, which gives rise to a reduction and eventual vanishing of the superfluid stiffness in the ground state.

ACKNOWLEDGMENTS

We thank I. Aleiner, B. Altshuler, E. Berg, D. Chowdhury, L. Classen, K. Efetov, R. Fernandes, A. Finkelstein, E. Fradkin, A. Georges, S. Hartnol, S. Karchu, S. Kivelson, I. Klebanov, A. Klein, R. Laughlin, S-S. Lee, G. Lonzarich, I. Esterlis, D. Maslov, F. Marsiglio, I. Mazin, M. Metlitski, W. Metzner, A. Millis, D. Mozyrsky, C. Pepan, V. Pokrovsky, N. Prokofiev, S. Raghu, S. Sachdev, T. Senthil, D. Scalapino, Y. Schattner, J. Schmalian, D. Son, G. Tarnopolsky, A-M Tremblay, A. Tsvelik, G. Torroba, E. Yuzbashyan, J. Zaanen, and particularly R. Combescot and Y. Wang for useful discussions. The work by A.V.C. and Y.M.W. was supported by the NSF Grant No. DMR-1834856. Y.-M.W, S.-S.Z., and A.V.C acknowledge the

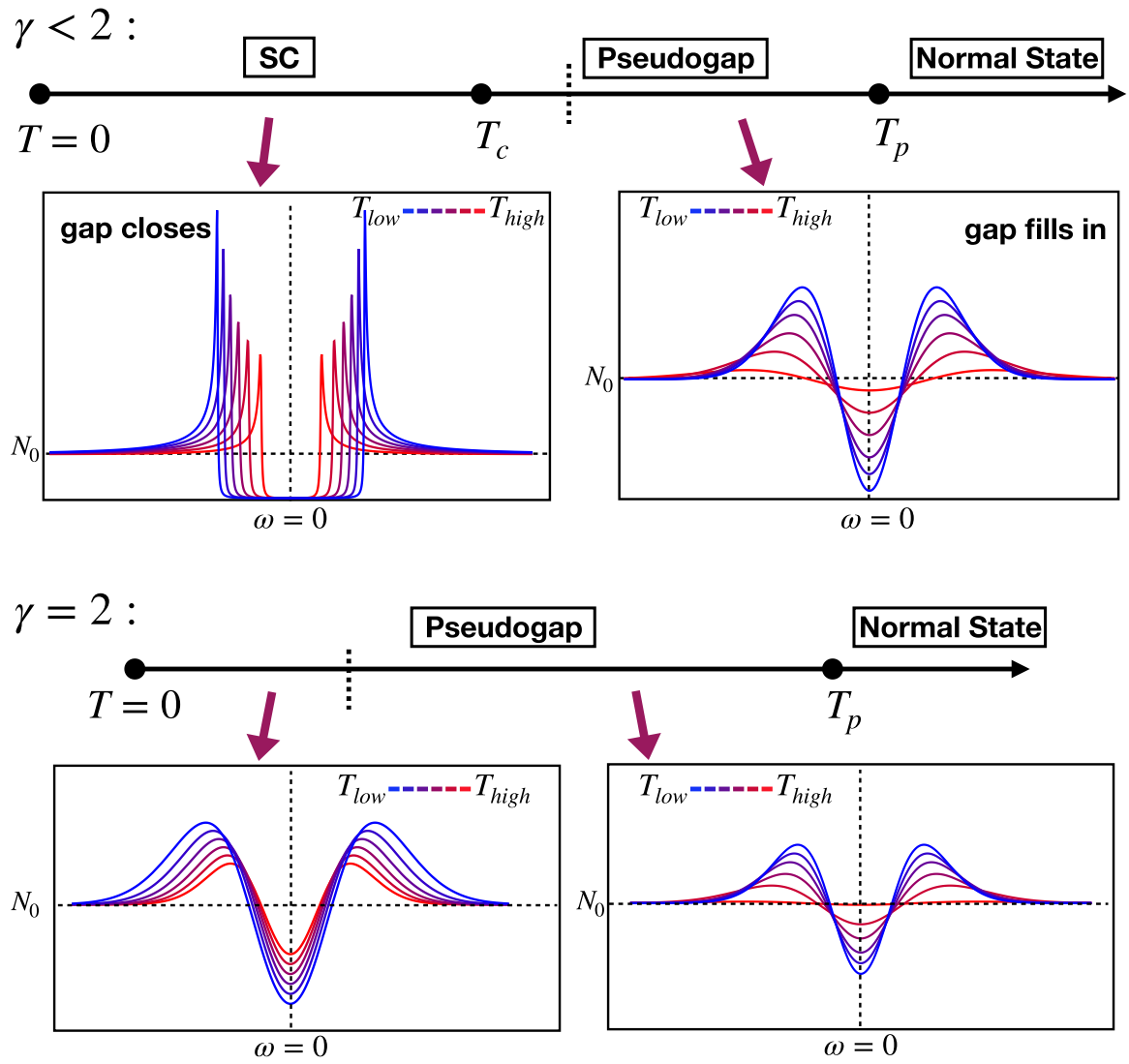

FIG. 18. The temperature evolution of the DoS $N(\omega)$. For $\gamma < 2$ (top), there is a SC order at $T < T_c$. In this regime and in the pseudogap state at $T \geqslant T_c$, the temperature variation of $N(\omega)$ resembles that in a conventional BCS superconductor, i.e. when T increases, the position of the maximum in $N(\omega)$ moves to a smaller frequency. At larger T within the pseudogap phase, $N(\omega)$ displays gap filling behavior when the peak position increases with increasing T and $N(\omega = 0)$ increases towards its normal state value. For $\gamma = 2$ (lower panel), $T_c = 0$, but the two different regimes of pseudogap behavior are present.

hospitality of KITP at UCSB, where part of the work has been conducted. The research at KITP is supported by the National Science Foundation under Grant No. NSF PHY-1748958. A.V.C. also acknowledges the hospitality of Stanford University, where some results of this work have been obtained. His stay at Stanford has been supported through the Gordon and Betty Moore Foundation's EPiQS Initiative, Grants No. GBMF4302 and No. GBMF8686.

APPENDIX A: EXPANSION IN $D^2(\omega_m)$ FOR $\gamma = 2$ AND $\gamma < 2$

In this Appendix, we present some details of the analysis of the nonlinear gap equation for $\gamma = 2$ and elaborate on the claim in the main text that a continuous set of gap functions exists only for $\gamma = 2$, while for smaller γ, the set is a discrete one.

1. $\gamma = 2$

We begin with $\gamma = 2$. Consider first the limit of small frequencies $\omega_m \ll \bar{g}$. For such ω_m, $\Delta(\omega_m)$ in the l.h.s. of the gap equation (4) can be neglected, as its inclusion leads to terms with extra $(\omega_m/\bar{g})^2$. This approximation is equivalent to neglecting ω_m compared to the self-energy $\Sigma(\omega_m)$ and is similar to the "no ω_m" approximation, used in the studies of SYK-type models [45–47]. The nonlinear gap equation at $T = 0$ without $\Delta(\omega_m)$ in the l.h.s reduces to

$$\int d\omega_{m'} \frac{D(\omega_{m'}) - D(\omega_m)}{\sqrt{1 + D^2(\omega_{m'})}} \frac{\mathrm{sgn}\omega'_m}{|\omega_m - \omega_{m'}|^2} = 0 \qquad \text{(A1)}$$

where, we recall, $D(\omega_m) = \Delta(\omega_m)/\omega_m$.

The linearized gap equation is obtained from (A1) by neglecting $D^2(\omega_{m'})$ in the denominator. The exact solution of the

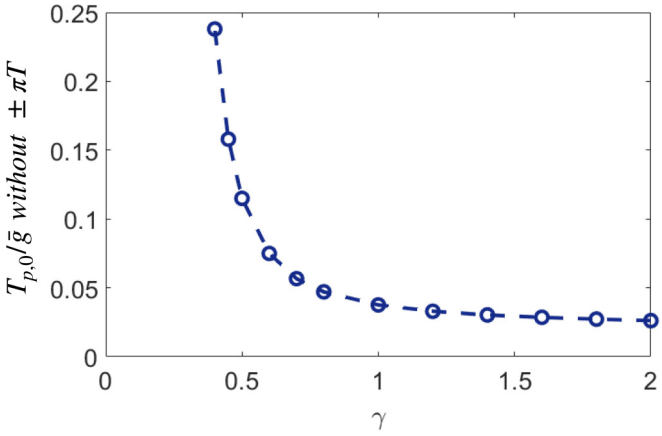

FIG. 19. The onset temperature of the pairing, obtained without including Matsubara frequencies $\omega_m = \pm\pi T$. For $\gamma = 2$, this temperature is roughly 1/7 of the actual $T_{p,0}$.

linearized gap equation is Eq. (13):

$$D(\omega_m) = 2\epsilon \cos\left(\beta \ln\left(\frac{|\omega_m|}{\bar{g}}\right)^2 + \phi_\epsilon\right)\mathrm{sgn}\omega, \tag{A2}$$

where ϵ is an arbitrary overall factor, ϕ_ϵ is yet undetermined constant, and $\beta = 0.38187$ satisfies $\pi\beta\tanh(\pi\beta) = 1$.

We now expand Eq. (A1) in powers of D^2. We will be searching for the solution in the form

$$D_\epsilon(\omega_m) = 2\sum_{n=0}^{\infty}\epsilon^{2n+1}Q_{2n+1} \times \cos\left((2n+1)\left(\beta_\epsilon \ln\left(\frac{|\omega_m|}{\bar{g}}\right)^2\right) + \phi_\epsilon\right). \tag{A3}$$

Substituting into (A1) and collecting contributions at each order in ϵ^{2n+1}, we find that $D_\epsilon(\omega_m)$ given by (A3) does satisfy Eq. (A1), and that all integrals are ultraviolet convergent, i.e., there is no need for regularization. The calculations are lengthy, but straightforward. We checked explicitly that β_ϵ is the same in all terms in (A3) and is related to the original β by

$$\beta_\epsilon = \beta\left(1 - \frac{\epsilon^2}{2} + 0.806\epsilon^4 + \cdots\right). \tag{A4}$$

The numerical coefficients are $Q_3 = 0.222 + O(\epsilon^2)$, $Q_5 = 0.043 + O(\epsilon^2)$. We cited this result and Eqs. (A3) and (A4) in Sec. III C.

At larger frequencies, we need to keep $\Delta(\omega_m)$ in the l.h.s. of (4). In the opposite limit $\omega_m \gg \bar{g}$, the leading term in $D_\epsilon(\omega_m)$ is obtained by pulling $1/\omega_m^2$ from the integrand in the r.h.s.. Then we obtain

$$D_\epsilon(\omega_m) = \frac{a_\epsilon}{\omega_m^3}, \tag{A5}$$

where

$$a_\epsilon = \frac{\bar{g}^2}{2}\int d\omega_{m'}\frac{D(\omega_{m'})}{\sqrt{1+D^2(\omega_{m'})}}\mathrm{sgn}\omega_m. \tag{A6}$$

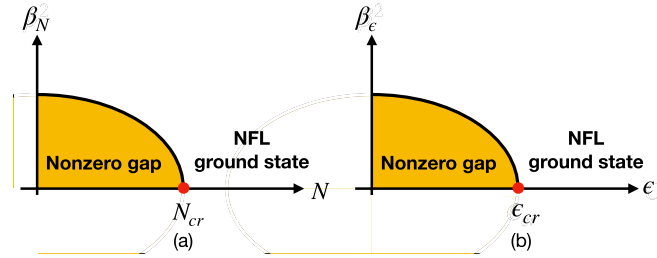

FIG. 20. The comparison between the behavior of β_ϵ in the $\gamma = 2$ model and β_N in the model with $\gamma < 1$, extended to $N > 1$.

Substituting this form of $D(\omega_m)$ into the integrand in the r.h.s, we find that the integral is ultra-violet convergent, i.e., the solution (A6) is self-consistent.

The two solutions have to merge at $\omega_m \sim \bar{g}$. For the linearized gap equation (the limit $\epsilon \to 0$), we verified that this does happen for a certain value of ϕ_ϵ in (A3). We conjecture that the same holds for other ϵ, i.e., for a certain ϕ_ϵ, $D_\epsilon(\omega_m)$ smoothly evolves between (A3) and (A6). We did similar analysis in paper I. There, we demonstrated that for arbitrary ϕ_ϵ, $D_\epsilon(\omega)$ of Eq. (A3) approaches the constant at $\omega_m \to \infty$, while the desired term ($D_\epsilon(\omega_m) \propto 1/|\omega_m|^{\gamma+1}$ for a generic γ) is the subleading one. For a particular ϕ_ϵ, a constant vanishes, and the high-frequency behavior becomes the expected one.

We see from (A4) that β_ϵ decreases with increasing ϵ, while the overall magnitude of $\Delta(\omega_m)$ increases. It is natural to expect that $\beta_\epsilon = 0$ at some critical $\epsilon = \epsilon_{\mathrm{cr}}$. We explored this in the main text.

Another way to argue for the existence of ϵ_{cr} is to depart from the opposite limit $\epsilon \gg 1$, where $D(\omega_m)$ is supposed to be large. In this case, we introduce $\Xi(\omega_m) = 1/D(\omega_m)$ and re-express the gap equation as

$$\int d\omega_{m'}\frac{\Xi(\omega_{m'}) - \Xi(\omega_m)}{\sqrt{1+\Xi^2(\omega_{m'})}}\frac{1}{|\omega_m - \omega_{m'}|^2} = 0 \tag{A7}$$

Note the absence of $\mathrm{sgn}\omega'_m$ in the integrand. At small Ξ, we neglect the $\Xi^2(\omega_{m'})$ in the denominator and search for the solution in the form $\Xi(\omega_m) = \mathrm{sgn}\omega_m|\omega_m/\bar{g}|^b$. Substituting into (A7) we find $b = \pm 1$, i.e.,

$$\Xi(\omega_m) = \left(A_1\frac{\bar{g}}{|\omega_m|} + A_2\frac{|\omega_m|}{\bar{g}}\right). \tag{A8}$$

The first term does not satisfy the normalization condition and has to be discarded (see paper I for the details on this). This leaves no parameter to adjust in order to match with the behavior at high frequencies. This implies that there is no solution for the gap at large ϵ.

There is a similarity between this analysis and the analysis in paper I, where we considered the γ model for $\gamma < 1$ and extended it using a continuous variable N to make interactions in the particle-hole and particle-particle channels nonequivalent. There, we found that there exists N_{cr}, which separates oscillating and nonoscillating solutions, and only oscillating solutions are compatible with high-frequency behavior. Here, ϵ plays the same role as N. We illustrate this in Fig. 20.

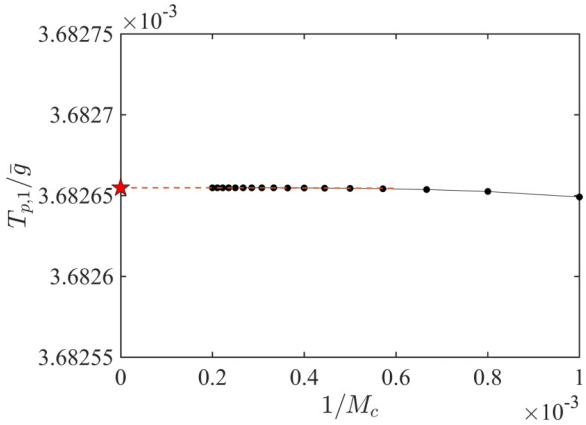

FIG. 21. Determination of the temperature $T_{p,1}$, at which the $n = 1$ solution develops in the $\gamma = 2$ model. $M_c \sim 10^3$ is the largest value of the Matsubara number, used in this numerical calculation. Extrapolating M_c to ∞ yields a finite value $T_{p,1} \simeq 3.6827\times10^{-3}\bar{g}$.

2. $\gamma < 2$

We now extend this approach to $\gamma < 2$. The gap equation for $D(\omega_m)$ at $\omega_m \ll \bar{g}$ has the same form as in (A1), only $|\omega_m - \omega_{m'}|^2$ in the denominator is replaced by $|\omega_m - \omega_{m'}|^\gamma$. The solution of the linearized equation for $D(\omega_m)$ is

$$D(\omega_m) = 2\epsilon\left(\frac{\bar{g}}{|\omega_m|}\right)^{1-\gamma/2}\cos\left(\beta_\gamma \ln\left(\frac{|\omega_m|}{\bar{g}}\right)^\gamma + \phi\right)\mathrm{sgn}\omega, \tag{A9}$$

where β_γ is some regular function of γ. As before, we search for the solutions in the form

$$D_\epsilon(\omega_m) = 2\sum_{n=1}^{\infty}\left(\epsilon\left(\frac{\bar{g}}{|\omega_m|}\right)^{1-\gamma/2}\right)^{2n+1} Q_{2n+1} \times \cos\left[(2n+1)\left(\beta_{\gamma,\epsilon}\ln\left(\frac{|\omega_m|}{\bar{g}}\right)^\gamma + \phi_\epsilon\right)\right]. \tag{A10}$$

Substituting into (A9), we find that the integrals that determine Q_{2n+1} now contain infra-red divergencies. The only way to eliminate the divergencies is to assume that Δ_ϵ tends to a finite value at $\omega_m \to 0$. But this is only possible for a discrete set of finite ϵ. We also note in passing that because the actual expansion parameter is $\epsilon(\bar{g}/|\omega_m|)^{1-\gamma/2}$, the expansion of $\beta_{\gamma,\epsilon}$ in powers of ϵ yields $\beta_{\gamma,\epsilon} = \beta_\gamma(1 + a(\epsilon(\bar{g}/|\omega_m|)^{1-\gamma/2})^2)$. For $a \neq 0$, this gives rise to additional terms, which are not matched by the terms in Eq. (A10). The only option then is to set $a = 0$, i.e., leave $\beta_{\gamma,\epsilon}$ equal to its bare value β_γ.

The outcome is that the continuous set of gap functions exists only for $\gamma = 2$. For smaller γ, this set is discrete. We also emphasize that the distinction between $\gamma = 2$ and $\gamma < 2$ holds only at $T = 0$. At any finite T, the set of gap functions is a discrete one for all $\gamma \leqslant 2$, and the solutions with different n from the set vanish at different temperatures $T_{p,n}$. In Fig. 21, we show the results of high-accuracy numerical calculation of $T_{p,1}$ for $\gamma = 2$. We see that $T_{p,1} \simeq 3.6827\times10^{-3}\bar{g}$ is finite.

APPENDIX B: THE GAP FUNCTION Δ_∞

The exact solution of the linearized gap equation at zero temperature has been derived for $0 < \gamma < 1$ in paper I and $1 < \gamma < 2$ in paper IV. Here we extend the analysis of paper IV to $\gamma = 2$.

We first solve for the gap function $\Delta_\infty(\omega_m)$ along the Matsubara axis. Following the same computational steps as in the analysis for $\gamma < 2$, we obtain $D_\infty(\omega_m) = \Delta_\infty(\omega_m)/\omega_m$ in the form

$$D_\infty(\omega_m) = \epsilon\frac{\bar{g}}{\omega_m}\int_{-\infty}^{\infty} dk b_k e^{-ik\ln(\omega_m/\bar{g})^2}, \tag{B1}$$

where ϵ is an infinitesimal number

$$b_k = \frac{e^{-iI_k}}{[\cosh(\pi(k-\beta))\cosh(\pi(k+\beta))]^{1/2}} \tag{B2}$$

and

$$I_k = \frac{1}{2}\int_{-\infty}^{\infty} dk' \ln|\epsilon_{k'} - 1|\tanh\pi(k' - k + i\delta), \tag{B3}$$

Here $\epsilon_{k'} = \pi k'\tanh(\pi k')$ and $\beta \simeq 0.38187$ is the solution of $\pi\beta\tanh(\pi\beta) = 1$. We cited these results in Eqs. (15)–(17) in the main text.

The integrals (B3) and (B1) can be computed numerically. We showed the result for $D_\infty(\omega_m)$ in Fig. 1 in the main text. The function $D_\infty(\omega_m)$ oscillates at $\omega_m < \bar{g}$ and decays as $1/|\omega_m|^3$ at $\omega_m > \bar{g}$.

1. Series expansion

The integral in Eq. (B3) can be evaluated by closing the integration contour along an infinite arc in the complex plane of frequency. For $|\omega_m| < \bar{g}$, the arc must be in the upper half-plane, and for $|\omega_m| > \bar{g}$, in the lower half-plane. The integral is equal to the sum of the contributions from each pole of the function b_k in the upper or lower half-plane. The position of these poles are obtained from the representation of b_k as an infinite product of the Gamma functions (see papers I and IV for details on this):

$$b_k = \frac{\Gamma(1-ik)}{\Gamma(1+ik)}\Gamma\left(\frac{1}{2} + i(k+\beta)\right)\Gamma\left(\frac{1}{2} + i(k-\beta)\right) \prod_{m=1}^{\infty}\frac{\Gamma\left(\frac{1}{2} + i(k - i\beta_m)\right)\Gamma(1+m-ik)}{\Gamma\left(\frac{1}{2} - i(k + i\beta_m)\right)\Gamma(1+m+ik)}. \tag{B4}$$

Here $\beta_m > 0$ are the solutions of $\pi\beta_m\tan(\pi\beta_m) = -1$. There is an infinite set of such β_m, specified by an integer $m = 0, 1, 2, \ldots$ Each β_m is located within the interval $1/2 + m < \beta_m < 3/2 + m$. Viewed as a function of complex k, b_k has poles from individual Γ functions in the upper half-plane at $k = \pm\beta + i(n + 1/2)$ and $k = i\beta_m + i(n + 1/2)$, $n, m = 0, 1, 2, \ldots$, and in the lower half-plane, at $k = -i(n + 1)$ and $k = -i(1 + m + n)$, where $n = 0, 1, 2, \ldots$ and $m = 1, 2, \ldots$.

2. $|\omega_m| < \bar{g}$

For $|\omega_m| < \bar{g}$, the relevant poles are at $k = \pm\beta + i(n + 1/2)$ and at $k = i\beta_m + i(n + 1/2)$, $n = 0, 1, 2, \ldots$. This yields

series expansion for $D_\infty(y)$ with $y = (|\omega_m|/\bar{g})^2$ in the form

$$D_\infty(y) = \mathrm{Re}\sum_{n=0}^{\infty} e^{(i\beta \ln y+\phi)} C_n^< y^n + \sum_{n,m=0}^{\infty} D_{n,m}^< y^{(n+\beta_m)}. \quad \text{(B5)}$$

The leading term in (B5) at small ω_m comes from the contribution of the poles at $k = \pm\beta + i/2$

$$D_\infty(y) = C_0^< \cos(\beta \ln y + \phi). \quad \text{(B6)}$$

The first subleading term comes from the contribution of the pole at $k = i(1/2 + \beta_0)$ and scales as y^{β_0}, where $\beta_0 \simeq 0.89$.

In the direct perturbation expansion in y, the series in y^n [the first term in (B5)] come from fermions with internal $y' \sim y$ and form the "local" series. The second term in (B5) is the sum of contributions from fermions with $y' = O(1)$, which for $y \ll 1$ can we regarded as "nonlocal". The total $D_\infty(y) = D_{\infty,L}(y) + D_{\infty,NL}(y)$.

The coefficients $C_n^<$ in (B5) can be obtained analytically, as we already found in papers I and III for $\gamma \leqslant 1$ and paper IV for $1 < \gamma < 2$. At $\gamma = 2$, the result takes a very simple form

$$C_n^< = C_0^< \frac{i^n}{\beta^n n!}. \quad \text{(B7)}$$

Substituting this into Eq. (B5), we find that the first term (the local contribution) becomes

$$D_{\infty,L}(y) \propto \cos[\beta(\ln y - y) + \phi]. \quad \text{(B8)}$$

It oscillates with the periodicity set by $\beta \ln y$ for $y \ll 1$, i.e., $|\omega_m| \ll \bar{g}$, which is the right behavior of the gap function at small frequencies, see (B6).

We note, however, that the first subleading term in (B8) scales as $y \sin(\beta \ln y)$. This contribution is smaller than the actual subleading term, which scales as $y^{0.89}$ and does not oscillate. This implies that, besides the leading term, the form of $\Delta_\infty(y)$ is determined by nonlocal corrections.

3. $|\omega_m| > \bar{g}$ and logarithmic correction

For $y > 1$, i.e., $|\omega_m| > \bar{g}$, relevant poles are in the lower half-plane. According to Eq. (B4), a pole at $k = -i(n+1)$ $(n = 0, 1, 2, \dots)$ is of order $n+1$, namely a simple pole at $n = 0$, a double pole at $n = 1$, etc. The leading term in the limit of $|\omega_m| \to \infty$ is the contribution from a simple pole at $k = -i$ $(n = 0)$, This contribution accounts for $1/y$ behavior of $\Delta_\infty(y)$ at large y. However, the subleading terms from the rest poles contain extra logarithms on top of powers of $1/y$:

$$\Delta_\infty(y) = \sum_{n=0}^{\infty} \tilde{C}_n^> \, y^{-2(1+n)} (\ln y)^n, \quad \text{(B9)}$$

To demonstrate the presence of the logs, consider as an example the contribution from the double pole at $k = -2i$. We shift γ to $2 - \delta$, $\delta > 0$ and then take the limit $\delta \to 0$. The expression for b_k for $\gamma \leqslant 2$ is presented in paper IV. Using it, we find that a double pole splits into two simple poles at $z_1 = -2i$ and $z_2 = -(2 + \delta/2)i$. In the neighborhood of the two poles, the function b_k takes the form $\sim 1/(z - z_1)/(z - z_2)$. The contribution from these two poles is obtained by circling out a loop $\mathcal{C}$ enclosing z_1 and z_2. Evaluating the integral and taking the limit $\delta \to 0$, we obtain

$$\sqrt{y} \lim_{\delta\to 0^+} \frac{\bar{g}}{\omega_m} \oint_{\mathcal{C}} dz \frac{1}{(z+2i)(z+(2+\delta/2)i)} e^{-iz\ln(y^{1-\delta/2})} = 2\pi \frac{\ln y}{y^2}. \quad \text{(B10)}$$

Similarly, the triple pole at $k = -3i$ gives rise to $(\ln y)^2/y^3$, etc. Collecting the contributions from every pole on the lower half-plane, we obtain (B9).

4. The universal oscillating term at large y

We now show that the high-frequency form of $D_\infty(\omega_m)$ contains an additional oscillating contribution. This contribution is exponentially small on the Matsubara axis, but, as we will see, it becomes the dominant one on the real axis. To extract this contribution, we note that for large $|\omega_m|/\bar{g}$, the argument of the cosine function, $I_k + k \ln y$, passes through extremum at $k \sim k_* = y/\pi$. Expanding around this point and evaluating the Gaussian integral, we obtain the universal piece $D_{\infty;u}(y)$ in the form

$$D_{\infty;u}(y) = 2\sqrt{2}\epsilon e^{-y} \cos\left[\frac{(\pi^2 - 2)}{2\pi} y + \frac{\pi}{4}\right]. \quad \text{(B11)}$$

We see that $D_{\infty;u}(y)$ is exponentially small, yet this oscillating term is present. The total $D_\infty(y)$ is the sum of (B9) and (B11).

5. $D_\infty(y)$ along real axis

Let's now transform from Matsubara to real axis. We use ω instead of y for better transparency. By construction, the gap function along the real axis is obtained by replacing $i\omega_m \to \omega + i0^+$ in the integrand in the r.h.s. of Eq. (B1). Under this transformation, $\ln(|\omega_m|/\bar{g})^2$ transforms into $\ln(|\omega|/\bar{g})^2 - i\pi$. The integral in Eq. (B1) splits into two parts:

$$D_\infty(\omega) = \epsilon \frac{\bar{g}}{\omega} \int_0^\infty dk \times \frac{e^{-\pi k} e^{-iI_k - ik\ln(|\omega|/\bar{g})^2} + e^{\pi k} e^{iI_k + ik\ln(|\omega|/\bar{g})^2}}{\sqrt{\cosh(\pi(k-\beta))\cosh(\pi(k+\beta))}}. \quad \text{(B12)}$$

Evaluating each integral by expanding near the point where $I_k \pm k\ln(|\omega|/\bar{g})^2$ passes through extremum and approximating the denominator in (B12) by its form at large k, we find that the first term is small in $e^{-2\pi k}$, while in the second term the exponential factor cancels out. Ignoring the first term, we obtain

$$D_{\infty;u}(\omega) \approx \sqrt{2}\epsilon e^{\frac{i}{\pi}[(\frac{\omega}{\bar{g}})^2 + \ln(\frac{\omega}{\bar{g}})^2]}. \quad \text{(B13)}$$

Other contributions to $D_\infty(\omega)$ contain powers of $\bar{g}/\omega$ and are smaller. As a result, on the real axis, $D_\infty(\omega) \approx D_{\infty;u}(\omega)$ at $\omega \gg \bar{g}$.

The same calculation can be carried out for an arbitrary complex frequency $z = \omega' + i\omega''$ in the upper frequency plane. For this, one has to replace $i\omega_m$ by $z \equiv |z|e^{i\psi}$ $(0 < \psi < \pi)$ in the integrand in the r.h.s. of (B1). This changes $\ln(|\omega_m|/\bar{g})^2$ to $\ln(|z|/\bar{g})^2 + i(2\psi - \pi)$ and gives $\Delta_\infty(z)$, which we presented in Eq. (62) in the main text.

APPENDIX C: EXTENDED γ MODEL

In papers I–III and other works [43,44,48–54], we and others extended the γ model to in-equal interactions in the particle-particle and particle-hole channels. This was done by adding a factor $1/N$ to the interaction in the particle-particle channel and leaving the interaction in the particle-hole channel intact. The advantage of extending the model to $N \neq 1$ is that superconducting order in the ground state exists for $N < N_{\rm cr}$, while for larger N the ground state is a non-Fermi liquid. By analyzing the gap equation near this point, one can obtain useful information about how a discrete set of solutions emerges. In paper III, we argued that the extension to $N \neq 1$ makes sense for $\gamma < 1$, while for $\gamma \geqslant 1$, the model with $N \neq 1$ possesses singularities, not present in the original γ model. We proposed another way to extend the model with $\gamma > 1$, which is free from singularities. The idea is to first explicitly cancel out singularities in the original γ model with $\gamma > 1$, and only then extend the model to $M \neq 1$ by making interactions in the particle-particle and particle-hole channel in-equivalent. The extended model is then free from singularities, and one can obtain critical $M_{\rm cr}$, where superconducting order disappears at $T = 0$ (by our construction, it exists at $M > M_{\rm cr}$). In this Appendix, we analyze the extended γ model for $\gamma = 2$. We show that a continuous set of solutions for the gap equation emerges at $M_{\rm cr} + 0$.

We first briefly describe the extension procedure. The two coupled Eliashberg equations are for the pairing vertex $\Phi(\omega_m)$ and the self-energy $\Sigma(\omega_m)$. For $\gamma = 2$, the equations are

$$\Phi(\omega_m) = \bar{g}^2 \pi T \sum_{m' \neq m} \frac{\Phi(\omega_{m'})}{\sqrt{\tilde{\Sigma}^2(\omega_{m'}) + \Phi^2(\omega_{m'})}} \frac{1}{|\omega_m - \omega_{m'}|^2},$$
$$\tilde{\Sigma}(\omega_m) = \omega_m + \bar{g}^2 \pi T \sum_{m' \neq m} \frac{\tilde{\Sigma}(\omega_{m'})}{\sqrt{\tilde{\Sigma}^2(\omega_{m'}) + \Phi^2(\omega_{m'})}} \frac{1}{|\omega_m - \omega_{m'}|^2}, \tag{C1}$$

where $\tilde{\Sigma}(\omega_m) = \omega_m + \Sigma(\omega_m)$. At $T = 0$, the r.h.s. of each of the two equations contains a divergent integral $\int dx/x^2$. To regularize the divergencies, we keep the temperature small but finite and set $T = 0$ at the end of calculations. At a finite T, the sum over m' is nonsingular as singular self-action term with $m' = m$ cancels out by the same reason as the contributions from nonmagnetic impurities.

We then introduce

$$\bar{\Phi}(\omega_m) = \Phi(\omega_m)\left(1 - \bar{g}^2 \frac{\zeta(2)}{(2\pi T)} \frac{1}{\sqrt{\tilde{\Sigma}^2(\omega_m) + \Phi^2(\omega_m)}}\right),$$
$$\bar{\tilde{\Sigma}}(\omega_m) = \tilde{\Sigma}(\omega_m)\left(1 - \bar{g}^2 \frac{\zeta(2)}{(2\pi T)} \frac{1}{\sqrt{\tilde{\Sigma}^2(\omega_m) + \Phi^2(\omega_m)}}\right). \tag{C2}$$

where $\zeta(2) = \pi^2/6 = \sum_{n=1}^{\infty} 1/n^2$. Because $\Phi(\omega_m)/\tilde{\Sigma}(\omega_m) = \bar{\Phi}(\omega_m)/\bar{\tilde{\Sigma}}(\omega_m)$, Eqs. (C1) can be re-expressed solely in terms of $\bar{\Phi}(\omega_m)$ and $\bar{\tilde{\Sigma}}(\omega_m)$:

$$\bar{\Phi}(\omega_m) = \bar{g}^2 \pi T \sum_{m' \neq m} \left(\frac{\bar{\Phi}(\omega_{m'})}{\sqrt{\bar{\tilde{\Sigma}}^2(\omega_{m'}) + \bar{\Phi}^2(\omega_{m'})}} - \frac{\bar{\Phi}(\omega_m)}{\sqrt{\bar{\tilde{\Sigma}}^2(\omega_m) + \bar{\Phi}^2(\omega_m)}} \right) \frac{1}{|\omega_m - \omega_{m'}|^2},$$
$$\bar{\tilde{\Sigma}}(\omega_m) = \omega_m + \bar{g}^2 \pi T \sum_{m' \neq m} \left(\frac{\bar{\tilde{\Sigma}}(\omega_{m'})}{\sqrt{\bar{\tilde{\Sigma}}^2(\omega_{m'}) + \bar{\Phi}^2(\omega_{m'})}} - \frac{\bar{\tilde{\Sigma}}(\omega_m)}{\sqrt{\bar{\tilde{\Sigma}}^2(\omega_m) + \bar{\Phi}^2(\omega_m)}} \right) \frac{1}{|\omega_m - \omega_{m'}|^2}. \tag{C3}$$

These equations are now free from singularities at $T = 0$, when the summation over Matsubara numbers is replaced by the integration over ω_m.

We now extend the modified Eliashberg equations (C3) by multiplying the interaction in the particle-particle channel by a factor $1/M$:

$$\bar{\Phi}(\omega_m) = \frac{\bar{g}^2}{2M} \int d\omega'_m \left(\frac{\bar{\Phi}(\omega'_m)}{\sqrt{\bar{\tilde{\Sigma}}^2(\omega'_m) + \bar{\Phi}^2(\omega'_m)}} - \frac{\bar{\Phi}(\omega_m)}{\sqrt{\bar{\tilde{\Sigma}}^2(\omega_m) + \bar{\Phi}^2(\omega_m)}} \right) \frac{1}{|\omega_m - \omega'_m|^2}. \tag{C4}$$

The gap function $\Delta(\omega_m)$ is expressed via $\bar{\Phi}(\omega_m)$ and $\bar{\tilde{\Sigma}}(\omega_m)$ in the same way as via the original $\Phi(\omega_m)$ and $\tilde{\Sigma}(\omega_m)$: $\Delta(\omega_m) = \omega_m \bar{\Phi}(\omega_m)/\bar{\tilde{\Sigma}}(\omega_m)$. The equation on $\Delta(\omega_m)$ is

$$\Delta(\omega_m) = \frac{\bar{g}^2}{2M} \int \frac{d\omega'_m}{|\omega_m - \omega'_m|^2} \left(\frac{\Delta(\omega'_m) - M \frac{\Delta(\omega_m)}{\omega_m} \omega'_m}{\sqrt{\Delta^2(\omega'_m) + (\omega'_m)^2}} - \frac{\Delta(\omega_m)(1 - M)}{\sqrt{\Delta^2(\omega_m) + \omega_m^2}} \right). \tag{C5}$$

Absorbing $1/M$ into $\bar{g}_M^2 = \bar{g}^2/M$, introducing a dimensionless $\bar{\omega}_m = \omega_m/\bar{g}_M$, $D(\bar{\omega}_m) = \Delta(\bar{\omega}_m)/\bar{\omega}_m$ and re-arranging, we obtain from (C5)

$$D(\bar{\omega}_m)\left(\bar{\omega}+\frac{1-M}{2}\int \frac{d\bar{\omega}'_m}{|\bar{\omega}_m-\bar{\omega}'_m|^2}\left(\frac{\mathrm{sgn}\bar{\omega}_m}{\sqrt{1+D^2(\bar{\omega}_m)}}-\frac{\mathrm{sgn}\bar{\omega}'_m}{\sqrt{1+D^2(\bar{\omega}'_m)}}\right)\right) = \frac{1}{2}\int \frac{d\bar{\omega}'_m}{|\bar{\omega}_m-\bar{\omega}'_m|^2}\frac{D(\bar{\omega}'_m)-D(\bar{\omega}_m)}{\sqrt{1+D^2(\bar{\omega}'_m)}}\mathrm{sgn}\bar{\omega}'_m. \tag{C6}$$

Both integrals in (C6) are free from singularities and infra-red convergent.

For infinitesimally small $D(\bar{\omega}_m)$, Eq. (C6) becomes

$$D(\bar{\omega}_m)\left(\bar{\omega}_m+\frac{1-M}{\bar{\omega}_m}\right) = \frac{1}{2}\int d\bar{\omega}'_m \frac{D(\bar{\omega}'_m)-D(\bar{\omega}_m)}{|\bar{\omega}_m-\bar{\omega}'_m|^2}\mathrm{sgn}\omega'_m, \tag{C7}$$

At small $\bar{\omega}_m$, the solution of the gap equation is

$$D(\bar{\omega}_m) = 2\epsilon\cos\left(\beta_M \ln\bar{\omega}_m^2+\phi\right)\mathrm{sgn}\omega_m, \tag{C8}$$

It has the same form as Eq. (13), but now $\beta_M^2 = M/\pi^2$. This form implies that $M_{\mathrm{cr}} = 0$.

We now assume that M is small and solve the nonlinear gap equation. Our key intension is to check whether we still have a continuum of solutions. For this purpose, it is sufficient to focus on small $\bar{\omega}_m$, when we can neglect bare $\bar{\omega}_m$ in the l.h.s. of (C6).

As in Sec. III C, we search for the solution of (C6) in the series in ϵ^2 for both $D(\bar{\omega}_m)$ and β. To leading order in M, we obtain

$$D(\bar{\omega}_m) = \frac{2\epsilon}{\pi}M^{1/2}\ln\bar{\omega}_m^2(1-3\epsilon^2+\cdots)^{1/2}, \tag{C9}$$

where dots stand for ϵ^4 and higher order terms. The $M^{1/2}$ dependence (same as $(M-M_{\mathrm{cr}})^{1/2}$ as $M_{\mathrm{cr}}=0$) is an expected one. The logarithmic dependence on frequency is consistent with the result in paper I, where we obtained $\ln\bar{\omega}_m^\gamma$ dependence at $N = N_{\mathrm{cr}}$. However, there such dependence exists only for $N = N_{\mathrm{cr}}$, while here we have an infinite set of solutions with the same frequency dependence, but different amplitudes, parametrized by ϵ. All solutions appear simultaneously at $M = 0+$.

A complimentary piece of evidence for multiple solutions comes about if we simplify the l.h.s. of (C6) by dropping D^2 terms in the denominator of the $(1-M)$ term. The gap equation then reduces to

$$D(\bar{\omega}_m)\left(\bar{\omega}+\frac{1-M}{2\bar{\omega}}\right) = \frac{1}{2}\int \frac{d\bar{\omega}'_m}{|\bar{\omega}_m-\bar{\omega}'_m|^2}\frac{D(\bar{\omega}'_m)-D(\bar{\omega}_m)}{\sqrt{1+D^2(\bar{\omega}'_m)}}\mathrm{sgn}\bar{\omega}'_m. \tag{C10}$$

The full gap equation for the original γ model is reproduced if we set $M = 1$, so Eq. (C10) can be viewed as another extension of the original model. The solution of the linearized gap equation is the same as before, with $\beta_M^2 = M/\pi$, hence $M_{\mathrm{cr}} = 0$. At $M \to 0$, the expansion in ϵ^2 now yields, to leading order in $M \equiv M - M_{\mathrm{cr}}$:

$$D(\bar{\omega}_m) = 2\epsilon\left(\cos f_M(\bar{\omega}_m)-\frac{\epsilon^2}{16M}\cos 3f_M(\bar{\omega}_m)+\cdots\right), \tag{C11}$$

where

$$f_M(\bar{\omega}_m) = \beta_{M,\epsilon}\ln\bar{\omega}_m^2+\phi \tag{C12}$$

and

$$\beta_{M,\epsilon}^2 = \beta_M^2\left(1-\frac{3\epsilon^2}{M}+\cdots\right). \tag{C13}$$

We see that the expansion holds in powers of ϵ^2/M and is valid up to $\epsilon \sim (M)^{1/2}$, at which $\beta_{M,\epsilon}^2$ vanishes. At larger ϵ, $\beta_{M,\epsilon}^2$ becomes negative, and the solution disappears (there is no normalized solution of the linearized gap equation). We see that there is again an infinite set of solutions, specified by ϵ, which runs between 0 and $\epsilon_{\mathrm{cr}} = O(\sqrt{M})$.

[1] A. Abanov and A. V. Chubukov, Interplay between superconductivity and non-fermi liquid at a quantum critical point in a metal. i. the γ model and its phase diagram at $T = 0$: The case $0 < \gamma < 1$, Phys. Rev. B **102**, 024524 (2020).

[2] Y.-M. Wu, A. Abanov, Y. Wang, and A. V. Chubukov, Interplay between superconductivity and non-fermi liquid at a quantum critical point in a metal. II. the γ model at a finite T for $0 < \gamma < 1$, Phys. Rev. B **102**, 024525 (2020).

[3] Y.-M. Wu, A. Abanov, and A. V. Chubukov, Interplay between superconductivity and non-fermi liquid behavior at a quantum critical point in a metal. iii. the γ model and its phase diagram across $\gamma = 1$, Phys. Rev. B **102**, 094516 (2020).

[4] Y.-M. Wu, S.-S. Zhang, A. Abanov, and A. V. Chubukov, Interplay between superconductivity and non-fermi liquid at a quantum critical point in a metal. iv. the γ model and its phase diagram at $1 < \gamma < 2$, Phys. Rev. B **103**, 024522 (2021).

[5] T.-H. Lee, A. Chubukov, H. Miao, and G. Kotliar, Pairing Mechanism in Hund's Metal Superconductors and the Universality of the Superconducting Gap to Critical Temperature Ratio, Phys. Rev. Lett. **121**, 187003 (2018).

[6] Y.-M. Wu, A. Abanov, and A. V. Chubukov, Pairing in quantum critical systems: Transition temperature, pairing gap, and their ratio, Phys. Rev. B **99**, 014502 (2019).

[7] A. Karakozov, E. Maksimov, and A. Mikhailovsky, The investigation of eliashberg equations for superconductors with strong electron-phonon interaction, Solid State Commun. **79**, 329 (1991).

[8] F. Marsiglio and J. P. Carbotte, Gap function and density of states in the strong-coupling limit for an electron-boson system, Phys. Rev. B **43**, 5355 (1991), for more recent results see F. Marsiglio and J. P. Carbotte, Electron-phonon superconductivity, in *The Physics of Conventional and Unconventional Superconductors*, edited by K. H. Bennemann and J. B. Ketterson (Springer-Verlag, Berlin, 2006) and references therein; F. Marsiglio, Annal. Phys. **417**, 168102 (2020).

[9] R. Combescot, Strong-coupling limit of Eliashberg theory, Phys. Rev. B **51**, 11625 (1995).

[10] Y. Wang, Solvable Strong-Coupling Quantum-Dot Model with a Non-Fermi-Liquid Pairing Transition, Phys. Rev. Lett. **124**, 017002 (2020).

[11] I. Esterlis and J. Schmalian, Cooper pairing of incoherent electrons: An electron-phonon version of the Sachdev-Ye-Kitaev model, Phys. Rev. B **100**, 115132 (2019).

[12] D. Hauck, M. J. Klug, I. Esterlis, and J. Schmalian, Eliashberg equations for an electron-phonon version of the Sachdev-Ye-Kitaev model: Pair breaking in non-fermi liquid superconductors, Ann. Phys. **417**, 168120 (2020).

[13] D. J. Scalapino, J. R. Schrieffer, and J. W. Wilkins, Strong-coupling superconductivity. I, Phys. Rev. **148**, 263 (1966); D. J. Scalapino, in *The Electron-Phonon Interaction and Strong-Coupling Superconductors, Superconductivity*, edited by R. D. Parks (Dekker, New York, 1969), p. 449.

[14] P. B. Allen and R. C. Dynes, Transition temperature of strong-coupled superconductors reanalyzed, Phys. Rev. B **12**, 905 (1975).

[15] G. Bergmann and D. Rainer, The sensitivity of the transition temperature to changes in $\alpha^2 f(\omega)$, Z. Physik **263**, 59 (1973).

[16] D. Rainer, Principles of ab initio calculations of superconducting transition temperatures, in *Progress in Low Temperature Physics* (Elsevier, Amsterdam, 1986), Chap. 4, pp. 371–424.

[17] P. Hertel, Die sprungtemperatur stark koppelnder supraleiter, Z. Phys. **248**, 272 (1971).

[18] V. T. Geilikman and N. F. Masharov, Influence of the form of the phonon spectrum on the transition temperature of superconductors, J. Low Temp. Phys. **6**, 131 (1972).

[19] A. Karakozov, E. Maksimov, and S. Mashkov, Effect of the frequency dependence of the electron-phonon interaction spectral function on the thermodynamic properties of superconductors, JETP **41**, 971 (1975).

[20] O. V. Dolgov, I. I. Mazin, A. A. Golubov, S. Y. Savrasov, and E. G. Maksimov, Critical Temperature and Enhanced Isotope Effect in the Presence of Paramagnons in Phonon-Mediated Superconductors, Phys. Rev. Lett. **95**, 257003 (2005).

[21] Y. Wang and A. Chubukov, Quantum-critical pairing in electron-doped cuprates, Phys. Rev. B **88**, 024516 (2013).

[22] F. Marsiglio, Eliashberg theory in the weak-coupling limit, Phys. Rev. B **98**, 024523 (2018).

[23] S. Mirabi, R. Boyack, and F. Marsiglio, Thermodynamics of eliashberg theory in the weak-coupling limit, Phys. Rev. B **102**, 214505 (2020).

[24] A. V. Chubukov, A. Abanov, I. Esterlis, and S. A. Kivelson, Eliashberg theory of phonon-mediated superconductivity – when it is valid and how it breaks down, Ann. Phys. **417**, 168190 (2020).

[25] C. A. R. Sá de Melo, M. Randeria, and J. R. Engelbrecht, Crossover from BCS to Bose Superconductivity: Transition Temperature and Time-Dependent Ginzburg-Landau Theory, Phys. Rev. Lett. **71**, 3202 (1993).

[26] D. J. Scalapino, S. R. White, and S. Zhang, Insulator, metal, or superconductor: The criteria, Phys. Rev. B **47**, 7995 (1993).

[27] L. Benfatto, A. Toschi, S. Caprara, and C. Castellani, Phase fluctuations in superconductors: From galilean invariant to quantum XY models, Phys. Rev. B **64**, 140506(R) (2001).

[28] L. Benfatto, S. Caprara, C. Castellani, A. Paramekanti, and M. Randeria, Phase fluctuations, dissipation, and superfluid stiffness in d-wave superconductors, Phys. Rev. B **63**, 174513 (2001).

[29] S. G. Sharapov, V. P. Gusynin, and H. Beck, Effective action approach to the Leggett's mode in two-band superconductors, Eur. Phys. J. B **30**, 45 (2002).

[30] A. V. Chubukov, I. Eremin, and D. V. Efremov, Superconductivity versus bound-state formation in a two-band superconductor with small fermi energy: Applications to fe pnictides/chalcogenides and doped $SrTiO_3$, Phys. Rev. B **93**, 174516 (2016).

[31] D. J. Scalapino, Y. Wada, and J. C. Swihart, Strong-Coupling Superconductor at Nonzero Temperature, Phys. Rev. Lett. **14**, 102 (1965).

[32] Y. Wada, The effect of quasiparticle damping on the ratio between the energy gap and the transition temperature of lead, Rev. Mod. Phys. **36**, 253 (1964).

[33] F. Marsiglio, M. Schossmann, and J. P. Carbotte, Iterative analytic continuation of the electron self-energy to the real axis, Phys. Rev. B **37**, 4965 (1988).

[34] J. P. Carbotte, F. Marsiglio, and B. Mitrović, Maximum $2\Delta_0/k_BT_c$ for electron-phonon superconductors, Phys. Rev. B **33**, 6135 (1986).

[35] J. Bardeen and M. Stephen, Free-energy difference between normal and superconducting states, Phys. Rev. **136**, A1485 (1964).

[36] R. Haslinger and A. V. Chubukov, Condensation energy in strongly coupled superconductors, Phys. Rev. B **68**, 214508 (2003).

[37] E. A. Yuzbashyan, A. V. Chubukov, A. Abanov, and B. L. Altshuler, Non BCS pairing near a quantum phase transition–effective mapping to a spin chain (unpublished).

[38] D. Mozyrsky and A. V. Chubukov, Dynamic properties of superconductors: Anderson-Bogoliubov mode and Berry phase in the BCS and BEC regimes, Phys. Rev. B **99**, 174510 (2019).

[39] J. Schrieffer, in *Theory of Superconductivity* (Benjamin, New York, 1964); V. J. Emery and S. A. Kivelson, Importance of phase fluctuations in superconductors with small superfluid density, Nature (London) **374**, 434 (1995).

[40] V. Pokrovsky, Properties of ordered, continuously degenerate systems, Adv. Phys. **28**, 595 (1979).

[41] K. Maki, The magnetic properties of superconducting alloys I, Phys. Phys. Fiz. **1**, 21 (1964).

[42] K. Maki, Theory of electron-spin resonance in gapless superconductors, Phys. Rev. B **8**, 191 (1973).

[43] A. Abanov, Y.-M. Wu, Y. Wang, and A. V. Chubukov, Superconductivity above a quantum critical point in a metal: Gap closing versus gap filling, Fermi arcs, and pseudogap behavior, Phys. Rev. B **99**, 180506(R) (2019).

[44] Y.-M. Wu, A. Abanov, Y. Wang, and A. V. Chubukov, Special role of the first Matsubara frequency for superconductivity near a quantum critical point: Nonlinear gap equation below T_c and spectral properties in real frequencies, Phys. Rev. B **99**, 144512 (2019).

[45] Y. Gu, A. Kitaev, S. Sachdev, and G. Tarnopolsky, Notes on the complex Sachdev-Ye-Kitaev model, J. High Energy Phys. 02 (2020) 157.

[46] A. A. Patel and S. Sachdev, Theory of a Planckian Metal, Phys. Rev. Lett. **123**, 066601 (2019).

[47] Y. Wang and A. V. Chubukov, Quantum phase transition in the Yukawa-Syk model, Phys. Rev. Res. **2**, 033084 (2020).

[48] S. Raghu, G. Torroba, and H. Wang, Metallic quantum critical points with finite BCS couplings, Phys. Rev. B **92**, 205104 (2015).

[49] Y. Wang, A. Abanov, B. L. Altshuler, E. A. Yuzbashyan, and A. V. Chubukov, Superconductivity Near a Quantum-Critical Point: The Special Role of the First Matsubara Frequency, Phys. Rev. Lett. **117**, 157001 (2016).

[50] H. Wang, S. Raghu, and G. Torroba, Non-fermi-liquid superconductivity: Eliashberg approach versus the renormalization group, Phys. Rev. B **95**, 165137 (2017).

[51] H. Wang, Y. Wang, and G. Torroba, Superconductivity versus quantum criticality: Effects of thermal fluctuations, Phys. Rev. B **97**, 054502 (2018).

[52] J. A. Damia, S. Kachru, S. Raghu, and G. Torroba, Two-Dimensional Non-Fermi-Liquid Metals: A Solvable Large-N Limit, Phys. Rev. Lett. **123**, 096402 (2019).

[53] A. V. Chubukov, A. Abanov, Y. Wang, and Y.-M. Wu, The interplay between superconductivity and non-Fermi liquid at a quantum-critical point in a metal, Ann. Phys. **417**, 168142 (2020).

[54] J. A. Damia, M. Solís, and G. Torroba, How non-fermi liquids cure their infrared divergences, Phys. Rev. B **102**, 045147 (2020).